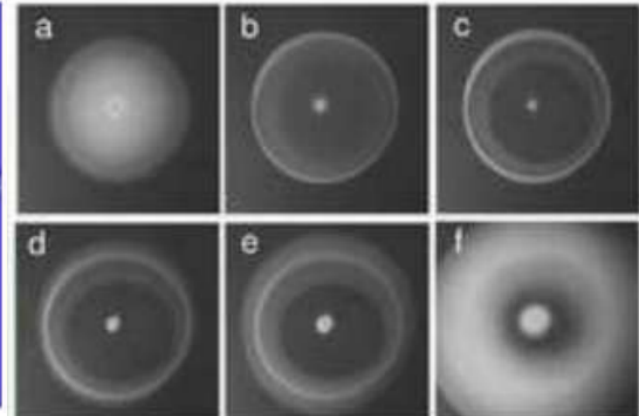
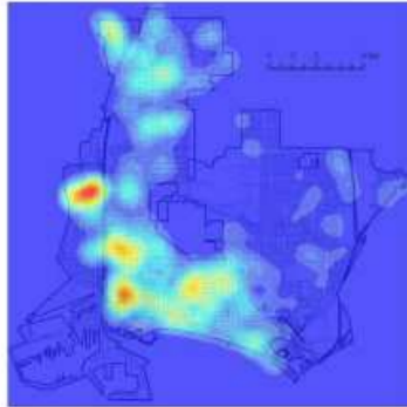


Spot solutions in Reaction-diffusion systems

seashells * vegetation * fish * crime hotspots in LA * stressed bacterial colony

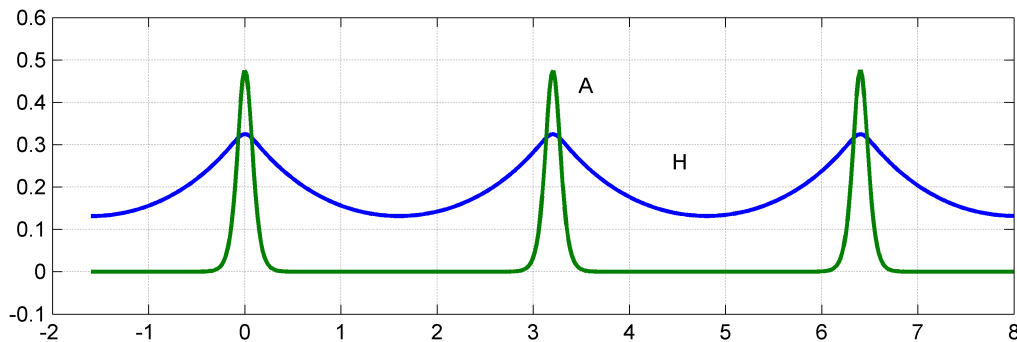


Classical Gierer-Meinhardt model

$$A_t = \varepsilon^2 \Delta A - A + \frac{A^2}{H}; \quad \tau H_t = D \Delta H - H + A^2$$

- Introduced in 1970's to model cell differentiation in hydra
- Mostly of mathematical interest: one of the simplest RD systems
- Has been intensively studied since 1990's [by mathematicians!]
- Key assumption: *separation of scales*

$$\varepsilon \ll 1 \text{ and } \varepsilon^2 \ll D.$$



Steady state (1D)

$$0 = \varepsilon^2 A_{xx} - A + \frac{A^2}{H}; \quad 0 = H_{xx} - H + A^2, \quad x \in \mathbb{R}$$

- Assume a spike at the center $x = 0$. Inner variables: $x = \varepsilon y$
- Inner expansion:

$$A_{yy} - A + A^2/H = 0, \quad H_{yy} \sim 0$$

$$H(y) \sim H_0,$$

$$A = H_0 w(y)$$

$$w_{yy} - w + w^2 = 0$$

$$w = \frac{3}{2} \operatorname{sech}^2(y/2)$$

- Outer:

$$H_{xx} - H + C_0\delta(x) = 0, \quad C_0 = \int_{-\infty}^{\infty} A^2(x)dx$$

$$H = \frac{C_0}{2} \exp(-|x|)$$

$$H_0 = \frac{C_0}{2}$$

$$\sim \frac{1}{2} \int A^2 dx$$

$$= \frac{\varepsilon}{2} H_0^2 \int w^2 dy$$

$$H_0 \sim \frac{2}{\varepsilon \int w^2 dy} = \frac{1}{3\varepsilon}$$

- Summary:

$$H_0 = \frac{1}{3\varepsilon}, \quad w(y) = \frac{3}{2} \operatorname{sech}^2(y/2);$$

$$A \sim H_0 w\left(\frac{x}{\varepsilon}\right), \quad H \sim H_0 \exp(-|x|)$$

- Questions: What about stability? What about location of the spike x_0 ?

“Classical” Results in 1D:

- Wei 97, 99, Iron+Wei+Ward 2000: Stability of K spikes in the GM model in one dimension
- Two types of possible instabilities: structural instabilities or translational instabilities
- Structural instabilities (large eigenvalues) lead to spike collapse in $O(1)$ time
- Translational instabilities can lead to “slow death”: spikes drift over large time scales
- **Main result 1:** There exists a sequence of thresholds D_K such that K spikes are stable iff $D < D_K$.
- **Main result 2:** Slow dynamics of K spikes is described by an ODE with $2K$ variables (spike heights and centers) subject to K algebraic constraints between these variables.

Large eigenvalues

- Careful derivation leads to a **nonlocal eigenvalue problem** (NLEP) of the form

$$\lambda\phi = \Delta\phi + (-1 + 2w)\phi - \chi w^2 \frac{\int w\phi}{\int w^2}; \quad \chi := \frac{4 \sinh^2\left(\frac{1}{\sqrt{D}}\right)}{2 \sinh^2\left(\frac{1}{\sqrt{D}}\right) + 1 - \cos[\pi(1 - 1/K)]}$$

- **Key theorem (Wei, 99):** $\text{Re}(\lambda) < 0$ iff $\chi < 1$
- **Corollary:** On a domain $[-1, 1]$, large eigenvalues are stable iff $D < D_{K,\text{large}}$ where

$$D_{K,\text{large}} = \frac{1}{\text{arcsinh}^2(\sin 2\pi/K)}$$

- When unstable, this can lead to **competition instability**.
- Movies: [stable](#); [unstable](#)

Small eigenvalues

- Causes a *very slow drift*
- Iron-Ward-Wei 2000: The slow dynamics of the system can be reduced to a coupled algebraic-differential system of ODEs
- Movie: [slow drift](#)

Two dimensions

- Structural stability is similar
- Dynamics [Ward et.al, 2000, K-Ward, 2004, K-Ward 2005]:

$$\frac{dx_0}{dt} \sim -\frac{4\pi\varepsilon^2}{\ln \varepsilon^{-1} + 2\pi R_0} \nabla R_0$$

where

$$R_0 = \lim_{x \rightarrow x_0} \left[G(x, x_0) + \frac{1}{2\pi} \ln(|x - x_0|) \right];$$

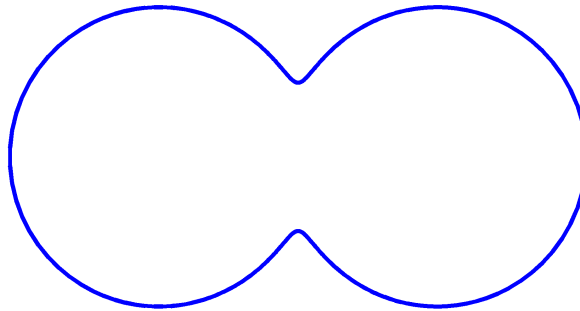
$$\nabla R_0 = \lim_{x \rightarrow x_0} \nabla_x \left[G(x, x_0) + \frac{1}{2\pi} \ln(|x - x_0|) \right];$$

$$\Delta G - \frac{1}{D}G = -\delta(x - x_0) \text{ on } \Omega; \quad \partial_n G = 0 \text{ on } \partial\Omega$$

- Equilibrium location x_0 satisfies $\nabla R_0 = 0$, occurs at the extremum of the regular part of the Neumann's Green's function

Dumbbell-shaped domain

- QUESTION: Suppose that a domain has a dumb-bell shape. Where will the spike drift??
- What are the possible equilibrium locations for a single spike?



Small D limit

- If D is very small, $R_0(x_0) \sim C(x_0) \exp\left(-\frac{1}{\sqrt{D}} |x_0 - x_m|\right)$ where x_m is the point on the boundary closest to x_0
- This means that R_0 is **minimized at the point furthest away from the boundary when $D \ll 1$**
 - In the limit $\varepsilon^2 \ll D \ll 1$, the spike drifts towards the point furthest away from the boundary.
 - For a dumbbell-shaped domain above, the three possible equilibria are at the "centers" of the dumbbells (stable) and at the center of the neck (unstable saddle point)
 - For multiple spikes, their locations solve "ball-packing problem".
- Movie: $D = 0.03, \varepsilon = 0.04$

Large D limit

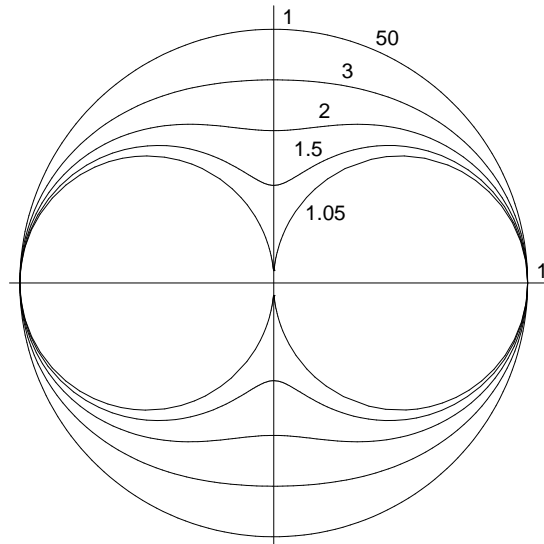
- We get the **modified Green's function**:

$$\Delta G_m - \frac{1}{|\Omega|} = -\delta(x - x_0) \text{ inside } \Omega, \quad \partial_n G = 0 \text{ on } \partial\Omega;$$

$$R_{m0} = \lim_{x \rightarrow x_0} \left[G_m(x, x_0) + \frac{1}{2\pi} \ln(|x - x_0|) \right].$$

- [K, Ward, 2003]: For a domain which is an analytic mapping of a unit disk, $\Omega = f(B)$, we derive an **exact formula** for ∇R_{m0} in terms of the residues of $f(z)$ outside the unit disk.

- Take $f(z) = \frac{(1 - a^2)z}{z^2 + a^2}$; $x_0 = f(z_0)$:



Then

$$\nabla R_{m0}(x_0) = \frac{\nabla s(z_0)}{f'(z_0)}$$

where

$$\nabla s(z_0) = \frac{1}{2\pi} \left(\begin{array}{l} \frac{z_0}{1-|z_0|^2} - \frac{(\bar{z}_0^2 + 3a^2)\bar{z}_0}{\bar{z}_0^4 - a^4} + \frac{a^2\bar{z}_0}{\bar{z}_0^2 a^2 - 1} + \frac{\bar{z}_0}{\bar{z}_0^2 - a^2} \\ - \frac{(a^4 - 1)^2 (|z_0|^2 - 1)(z_0 + a^2\bar{z}_0)(\bar{z}_0^2 + a^2)}{(a^4 + 1)(\bar{z}_0^2 a^2 - 1)(z_0^2 - a^2)(\bar{z}_0^2 - a^2)^2} \end{array} \right)$$

- Corollary: for above Ω , ∇R_{m0} has a unique root at the origin!
 - In the limit $D \gg 1$, all spikes will drift towards the neck.
- Complex bifurcation diagram as D is increased.
- Movie: $\varepsilon = 0.05$, $D = 0.1$; $D = 1$.

”Huge” D

- In the limit $D \rightarrow \infty$, (Shadow limit), an interior spike is unstable and moves towards the boundary [Iron Ward 2000; Ni, Poláčik, Yanagida, 2001].
- For **exponentially large but finite** $D = O(\exp(-C/\varepsilon))$, boundary effects will compete with the Green’s function.
- [K, Ward, 2004]: Define

$$\sigma := \frac{\varepsilon}{2} \ln \left(\frac{C_0}{|\Omega|} D \varepsilon^{-1/2} \right); \quad C_0 \approx 334.80;$$

Then the spike will move towards the boundary whenever its distance from the closest point of the boundary is at most σ ; otherwise it will move away from the boundary.

- Movies: $\varepsilon = 0.05$, $D = 10$; $D = 100$

Spike dynamics inside a disk

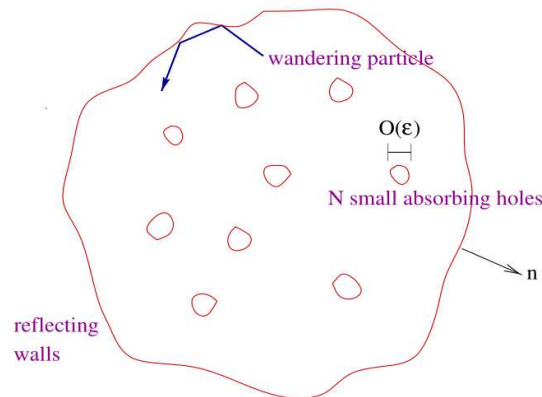
In the limit $\varepsilon \ll 1, D \gg 1$, inside the disk we get

$$C \frac{dx_j}{dt} \sim \underbrace{2 \sum_{k \neq j} \frac{x_j - x_k}{|x_j - x_k|^2} - \sum_k x_j}_{\text{inter - particle force}} + \underbrace{\sum_k \frac{x_j - x_k / |x_k|^2}{|x_j - x_k / |x_k|^2|^2} - \sum_k \frac{-x_j |x_k|^2 + x_k |x_j|^2}{|x_j |x_k|^2 - x_k|^2}}_{\text{reflection in the boundary of unit disk}}.$$

- The first two terms are identical to vortex stability model!
- The last two terms represent “reflection in the wall”
- Just like for vortex model, ***the steady state consists of uniformly-distributed particles inside the domain!***
- Movies: [disk](#); [dumbbell](#).

Mean first passage time (ice fishing)

- Question: Suppose you want to catch a fish in a lake covered by ice. Where do you drill a hole to maximize your chances?
- Related questions: cell signalling; oxygen transport in muscle tissues; cooling rods in a nuclear reactor...
- Consider N non-overlapping small "holes" each of small radius ε . A particle is performing a random walk inside the domain Ω . If it hits a hole, it gets destroyed; if it hits a boundary, it gets reflected. Question: what is the expected lifetime of the wandering particle? How do we place the holes to minimize this lifetime [i.e. catch the fish, cool the nuclear reactor...]?



- The expected lifetime is proportional to $1/\lambda$ where λ is the smallest eigenvalue of the problem:

$$\Delta u + \lambda u = 0 \text{ inside } \Omega \setminus \Omega_p; \quad u = 0 \text{ on } \partial\Omega_p; \quad \partial_n u = 0 \text{ on } \partial\Omega$$

where $\Omega_p = \bigcup_{i=1}^N \Omega_\varepsilon$.

- [K-Ward-Titcombe, 2005]: The smallest eigenvalue is given by

$$\lambda \sim \frac{2\pi N}{\ln \frac{1}{\varepsilon}} \left(1 - \frac{2\pi}{\ln \frac{1}{\varepsilon}} p(x_1, \dots, x_N) + O\left(\frac{1}{(\ln \frac{1}{\varepsilon})^2}\right) \right)$$

where

$$p(x_1, \dots, x_N) := \sum \sum G_{ij};$$

$$G_{ij} = \begin{cases} G_m(x_i, x_j) & \text{if } i \neq j \\ R_m(x_i, x_i) & \text{if } i = j \end{cases}$$

$$\Delta G_m(x, x') - \frac{1}{|\Omega|} = -\delta(x - x') \text{ inside } \Omega, \quad \partial_n G = 0 \text{ on } \partial\Omega; \quad R_m \equiv \text{reg. part}$$

- For a unit disk:

$$2\pi G_m(x, x') = -\ln |x - x'| - \ln \left| x |x'| - \frac{x'}{|x'|} \right| + \frac{1}{2} (|x|^2 + |x'|^2)$$

$$2\pi R_m(x, x') = -\ln \left| x |x'| - \frac{x'}{|x'|} \right| + \frac{1}{2} (|x|^2 + |x'|^2)$$

- The optimum trap placement is at the minimum of $p(x_1, \dots, x_N)$

Disk domain, N holes

We need to minimize

$$p(x_1 \dots x_N) = - \sum_{j \neq k} \ln |x_j - x_k| - \sum_{j,k} \left(\ln \left| x_j - \frac{x_k}{|x_k|^2} \right| + \ln |x_k| \right) + \frac{1}{2} \sum_{j,k} (|x_j|^2 + |x_k|^2)$$

Gradient flow is uniform swarm model plus two extra terms

$$\frac{dx_j}{dt} = 2 \sum_{k \neq j} \frac{x_j - x_k}{|x_j - x_k|^2} - \sum_k x_j + \sum_k \frac{x_j - x_k / |x_k|^2}{|x_j - x_k / |x_k|^2|^2} - \sum_k \frac{-x_j |x_k|^2 + x_k |x_j|^2}{|x_j |x_k|^2 - x_k|^2}.$$

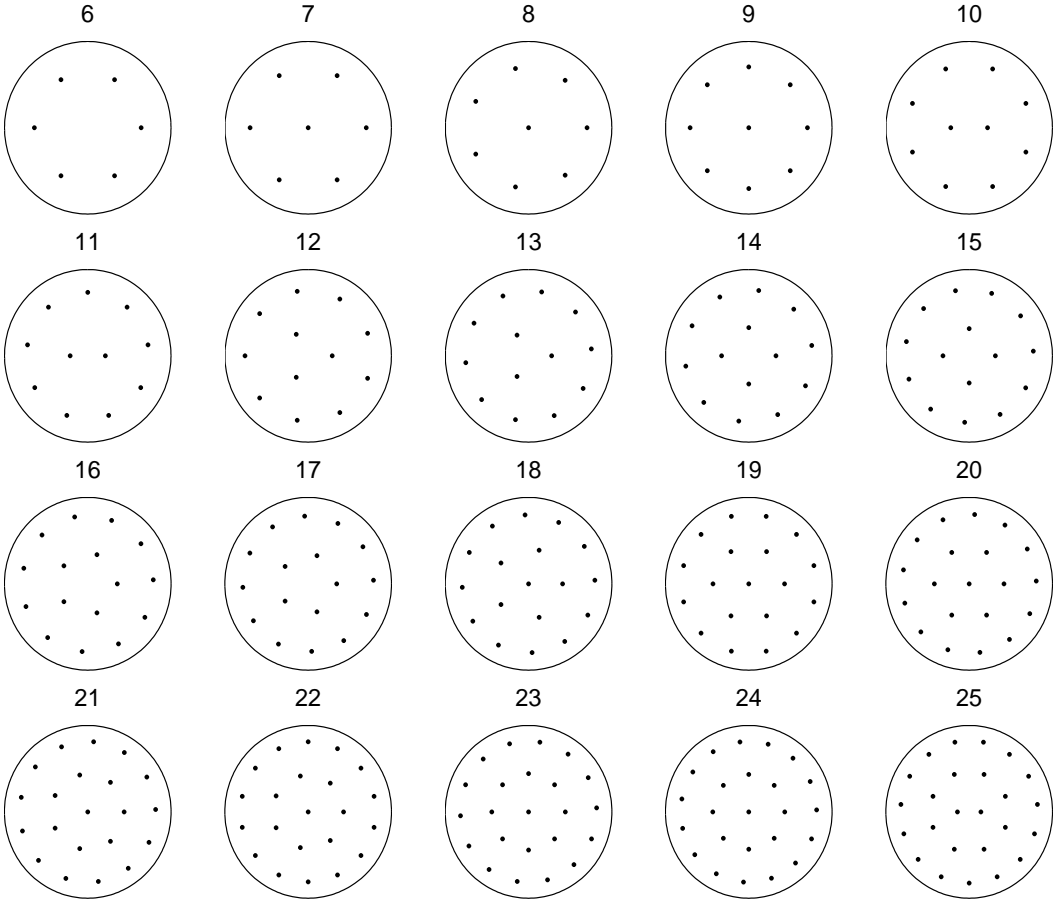
Particles on a ring: $x_k = r e^{ik2\pi/N}$. The min occurs when

$$\frac{r^{2N}}{1 - r^{2N}} = \frac{N - 1}{2N} - r^2$$

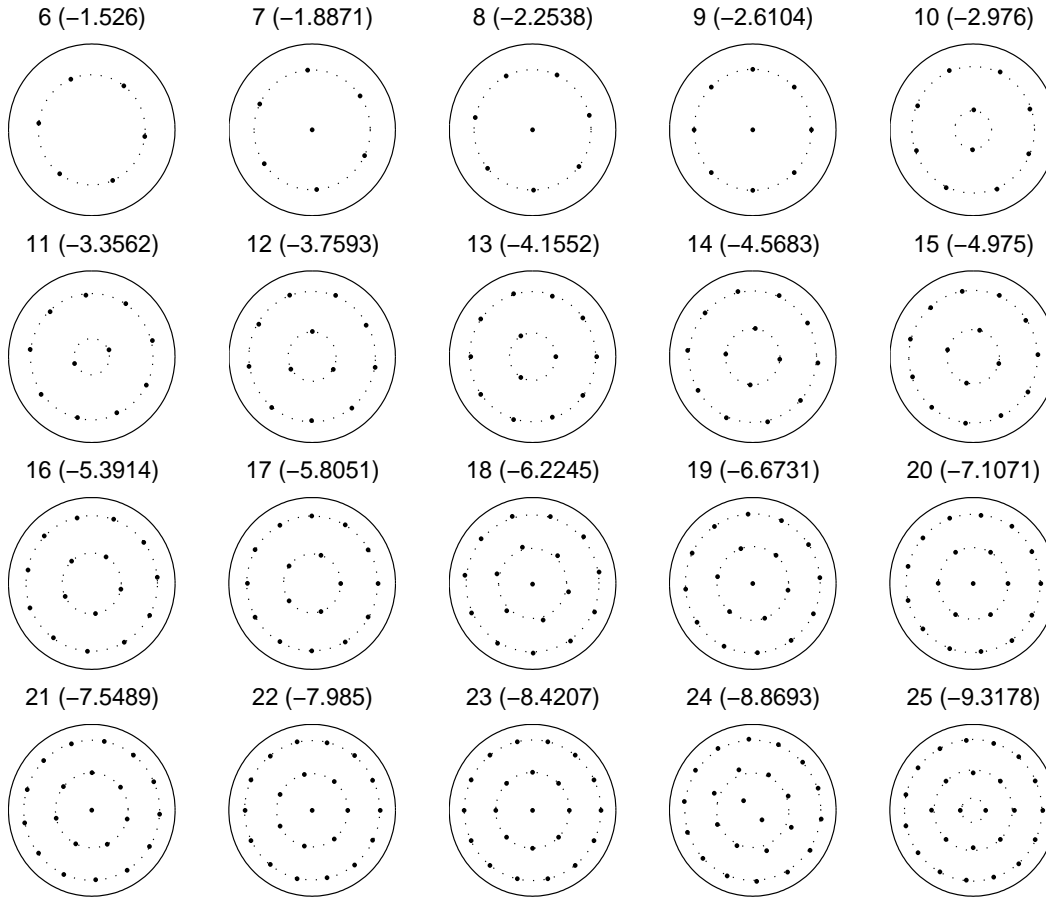
Note that $r \rightarrow 1/\sqrt{2}$ as $N \rightarrow \infty$; the optimal ring divides the unit disk into two equal areas.

Particles on 2,3,... m rings: Similar results are derived with complicated but numerically useful formulas.

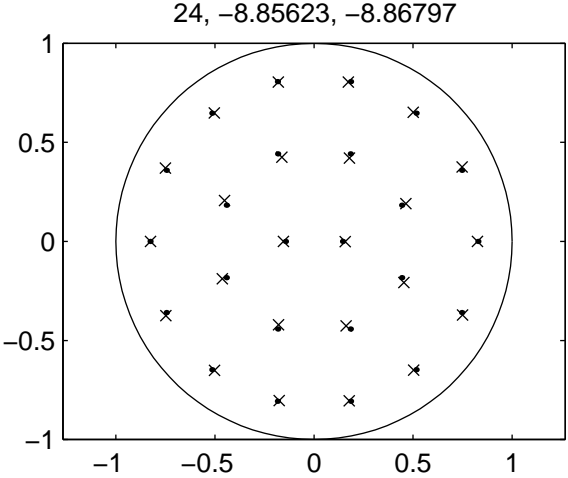
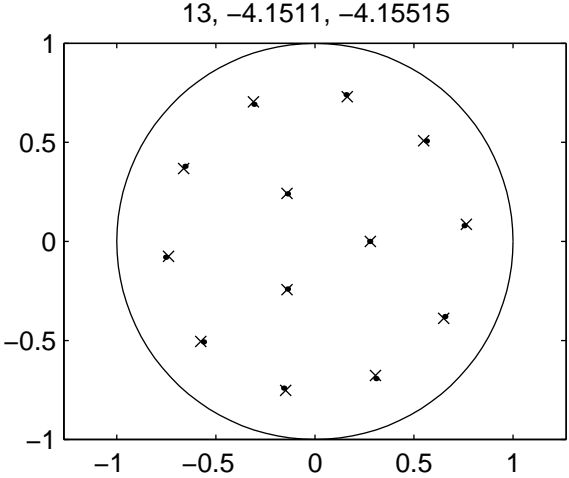
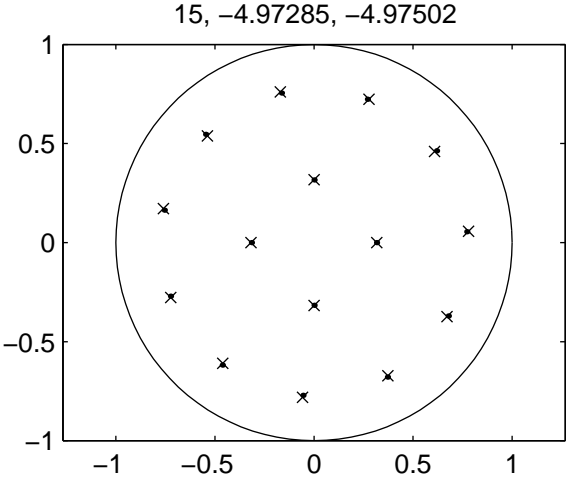
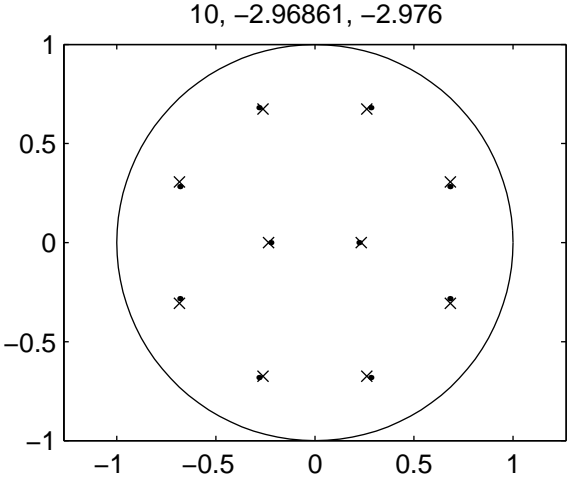
Constrained optimization on up to 3 rings



Full optimization of K traps



Comparison



Entire solutions to GM in higher dimensions

$$0 = \varepsilon^2 \Delta A - A + \frac{A^2}{H}; \quad 0 = \Delta H - H + A^2$$

- **Open question:** Does a spike solution exist in all of \mathbb{R}^3 ??
 - In 1D or 2D, there is separation of scales so YES. The inner problem is the ground state

$$\Delta w - w + w^2 = 0$$

- **Open question:** Does a spike solution exist in all of \mathbb{R}^3 ??
 - In 3D, the inner problem is **fully coupled**, the core problem becomes

$$0 = \Delta A - A + \frac{A^2}{H}; \quad 0 = \Delta H + A^2$$

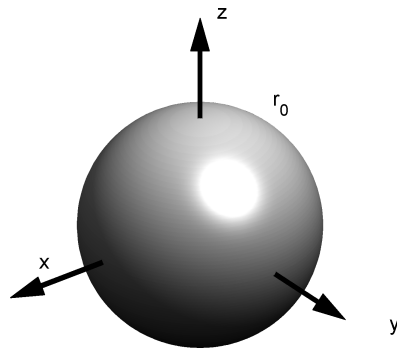
- **Open question:** Does a spike in 3D exist???

Solutions concentrating on spheres in \mathbb{R}^3

- Consider a general GM model:

$$0 = \varepsilon^2 \Delta A - A + \frac{A^p}{H^q}; \quad 0 = \Delta H - H + \frac{A^m}{H^s}.$$

- [Ni-Wei 2006, K-Wei, 2006] Shell-solutions: Seek solutions where A concentrates on a surface of a sphere of radius r_0 .



$$A(x) \sim Cw \left(\frac{|x| - r_0}{\varepsilon} \right)$$

where w is the 1D ground state: $w_{yy} - w + w^2 = 0$; $w = \frac{3}{2} \operatorname{sech}^2(y/2)$.

- In 3D, the radius of the sphere satisfies

$$\frac{p-1}{q} \sim \frac{e^{2r_0} - 1 - r_0}{e^{2r_0} - 1} \quad \text{as } \varepsilon \rightarrow 0$$

- Note that $\frac{p-1}{q} \rightarrow 1$ as $r_0 \rightarrow \infty$.

- The "standard GM"

$$\varepsilon^2 \Delta A - A + A^2/H = 0 = \Delta H - H + A^2 \quad (1)$$

has $(p, q, m, s) = (2, 1, 2, 0)$ is a degenerate case ($p+1 = q, r_0 \rightarrow \infty$)

- [K-Wei, 2012] For (1) we have

$$\varepsilon \sim \exp(-2r_0) (1 + 2r_0) \frac{70}{103} \quad (2)$$

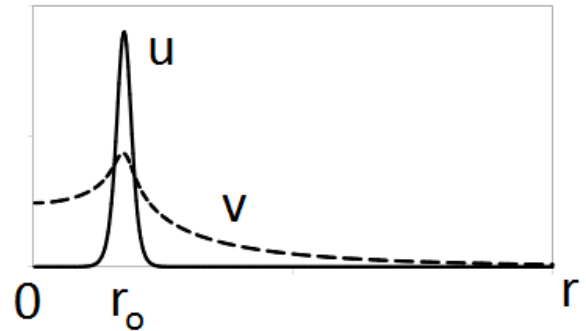
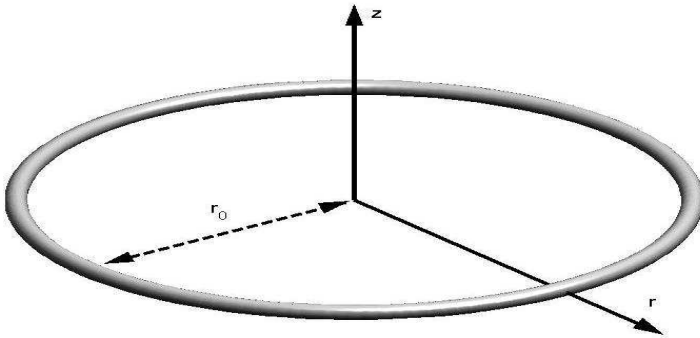
- The computation to get (2) is about 10 pages.

- Roughly, $r_0 \sim -\frac{1}{2} \ln \varepsilon \rightarrow \infty$ as $\varepsilon \rightarrow 0$.

Smoke-ring solutions

Axi-symmetric ansatz:

$$A(x, y, z) = u(r, z), \quad H(x, y, z) = v(r, z) \quad \text{where } r = \sqrt{x^2 + y^2}$$



The GM model becomes:

$$0 = \varepsilon^2 \left(\Delta_{(r,z)} u + \frac{1}{r} u_r \right) - u + \frac{u^p}{v^q}; \quad 0 = \left(\Delta_{(r,z)} v + \frac{1}{r} v_r \right) - v + \frac{u^m}{v^s} \quad (3)$$

Theorem Suppose that $q = p - 1$. Then the (3) admits a solution of the form

$$u \sim Cw(R); \quad R = \frac{\sqrt{(r - r_0)^2 + z^2}}{\varepsilon}$$

where w is a 2D ground state:

$$w_{RR} + \frac{1}{R}w_R - w + w^p = 0; \quad w'(0) = 0; \quad w > 0$$

and the radius r_0 given implicitly by

$$1 - 2r_0 \int_0^1 \frac{e^{-2r_0 t}}{\sqrt{1-t^2}} dt = \frac{1}{2}(m - s - 1) \frac{\int_0^\infty w^m \left(\int_0^R w^{p+1} t dt \right) R dR}{\left(\int_0^\infty w^m R dR \right) \left(\int_0^\infty w^{p+1} R dR \right)}. \quad (4)$$

The solution to (4) is always unique It exists if $m - s - 1 \leq 2$.

Some key steps in derivation

- Need to compute the axi-symmetric Green's function:

$$\Delta G + \frac{1}{r}G_r - G = -\delta(x, x_0).$$

- **Descent from 3D:** G is a convolution of the 3D Green's function $\Gamma(x, x') = \frac{e^{-|x-x'|}}{4\pi|x-x'|}$ along a ring of radius r_0 :

$$G(r, z, r_0, z_0) = \frac{r_0}{4\pi} \int_0^{2\pi} \frac{\exp[-(r^2 + r_0^2 - 2rr_0 \cos \omega + (z - z_0)^2)^{1/2}]}{4\pi(r^2 + r_0^2 - 2rr_0 \cos \omega + (z - z_0)^2)^{1/2}} d\omega$$

- Asymptotically **expand the singular integral** as $r \rightarrow r_0$
- Expand the steady state in **two scales:** ε and $\ln \varepsilon$.
- Higher-order solvability condition at $O(\varepsilon \ln \varepsilon)$.

Wave propagation through complex geometry

- Motivation:

PHYSICAL REVIEW E 73, 036219 (2006)

Guiding chemical pulses through geometry: Y junctions

L. Qiao and I. G. Kevrekidis*

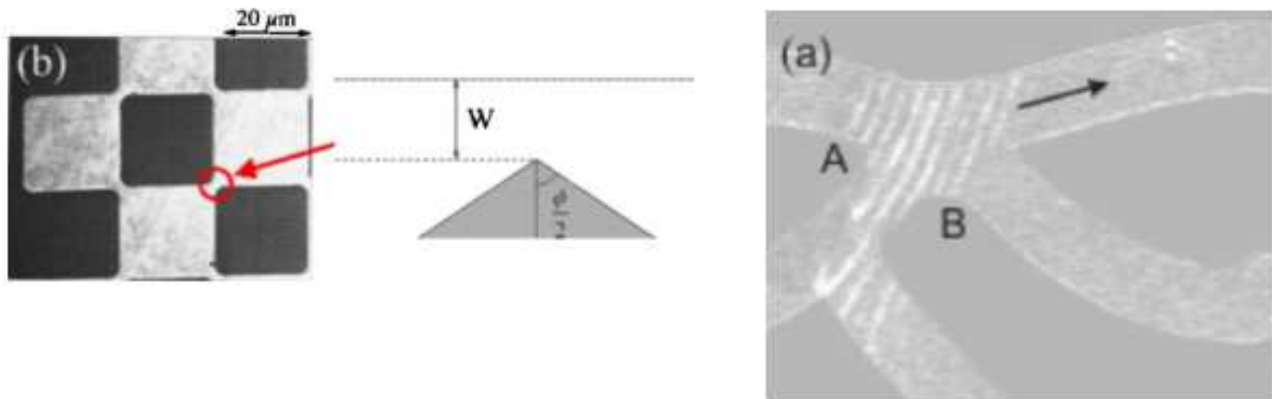
Department of Chemical Engineering, Princeton University, Princeton, New Jersey 08544, USA

C. Punckt and H. H. Rotermund

Fritz-Haber-Institut der MPG, Faradayweg 4-6, 14195 Berlin, Germany

(Received 8 December 2005; published 29 March 2006)

We study computationally and experimentally the propagation of chemical pulses in complex geometries. The reaction of interest, CO oxidation, takes place on single crystal Pt(110) surfaces that are microlithographically patterned; they are also *addressable* through a focused laser beam, manipulated through galvanometer mirrors, capable of locally altering the crystal temperature and thus affecting pulse propagation. We focus on sudden changes in the domain shape (corners in a Y-junction geometry) that can affect the pulse dynamics; we also show how brief, localized temperature perturbations can be used to control reactive pulse propagation. The computational results are corroborated through experimental studies in which the pulses are visualized using reflection anisotropy microscopy.



Perturbed Allen-Cahn model

$$u_t = \varepsilon^2 \Delta u - 2(u - \varepsilon a)(u - 1)(u + 1), \quad x \in \Omega \subset \mathbb{R}^2; \quad \partial_n u = 0 \text{ on } \partial\Omega$$

- Standard Allen-Cahn corresponds to $a = 0$:
 - In 1-D, the steady state is given by $u = \pm \tanh(x/\varepsilon)$.
 - In 2-D, the profile is 1-dimensional in some direction; the zero set $u = 0$ is a straight line, intersects boundary transversally.
 - Such straight interface is stable (unstable) provided it is a local min (max) of the distance function. [Kowalczyk, 05]
 - Time dependent solution evolves by mean curvature law until the interface merges with the boundary or becomes straight. [RSK, 89]
- When $a \neq 0$, the evolution of the equilibrium solution has a **curvature** \hat{R}^{-1} where

$$\hat{R} = \frac{1}{2a}.$$

- Sometimes the interface gets stuck in a narrow channel, other times it passes through:

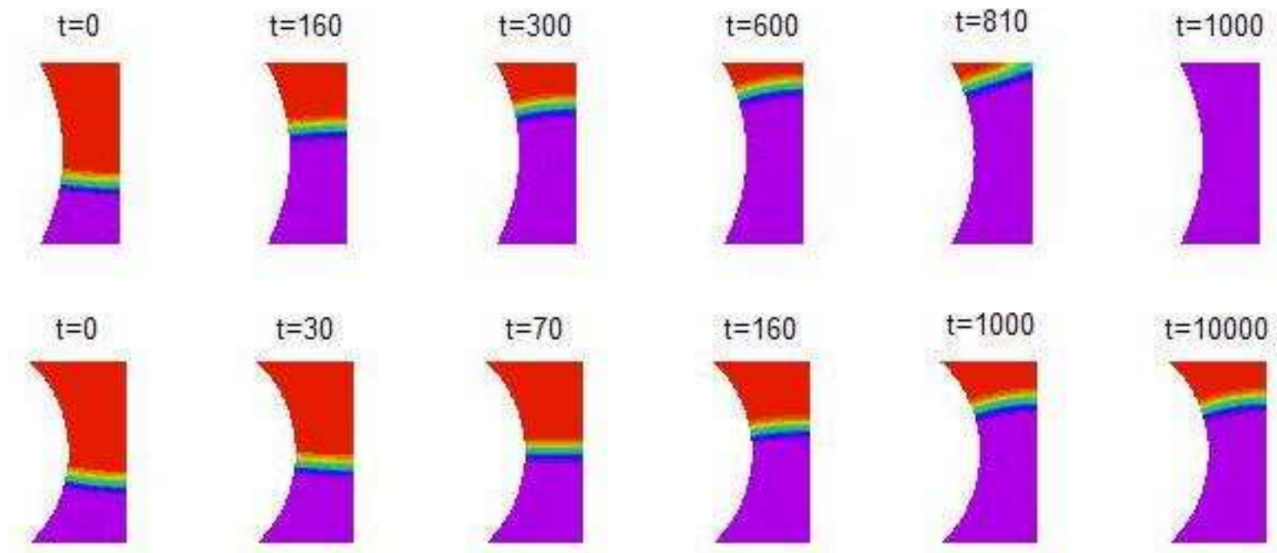


FIG. 1.1. Motion of an interface for the perturbed Allen Cahn model given by $u_t = \varepsilon^2 \Delta u - 2(u - \varepsilon a)(u^2 - 1)$, with $a = 0.3, \varepsilon = 0.07$. Top row: the interface is unstable and eventually disappears. Bottom row: The interface gets “stuck” in the middle of the domain; a non-trivial equilibrium is reached. The domain height is 1.5 and the distance between the side boundaries is 0.5. The radius of the left boundary is 1.5 for the top row and 1.0 for the bottom row.

- [Movie: stuck](#) [Movie: unstuck](#)

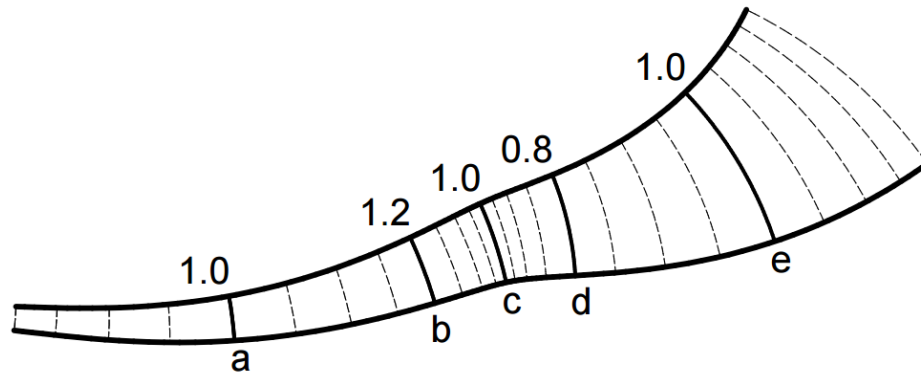
- In [K-iron-Rumsey-Wei, 2008] we classify the stability of such an interface.

- Main result: Eigenvalues satisfy the ***geometric eigenvalue problem***,

$$\begin{cases} w_{zz} - \hat{R}^{-2}w = -\lambda_0 w; \\ w'(-l/2) + \kappa_- w(-l/2) = 0; \\ w'(l/2) + \kappa_+ w(l/2) = 0; \end{cases}$$

where l is the interface length; κ_- , κ_+ are the two curvatures of the boundary at the points where the interface intersects it.

- Geometric criterion:



Stability $\iff R'(s) < 0$ whenever $R = \hat{R}$

Example: If $\hat{R} = 1$ then curve c represents the location of a stable interface, whereas curves a and e correspond to unstable interfaces.

Layer oscillations

- FitzHuhg-Nagumo type model:

$$u_t = \varepsilon^2 u_{xx} + 2(u - u^3) + w, \quad \tau w_t = Dw_{xx} - u + \beta$$

Neumann BC on $[0, 1]$

$$\varepsilon \ll 1, \quad D \gg 1$$

- Stationary steady state is an interface computed from the shadow limit $D \rightarrow \infty$

$$w \sim 0; \quad u \sim \tanh\left(\frac{l_0 - x}{\varepsilon}\right); \quad l_0 := (1 + \beta)/2$$

- [McKay-K]: As τ is increased, the interface is destabilized via a Hopf Bifurcation ([movie1](#), [movie2](#)). The critical scaling is:

$$\tau = \frac{D}{\varepsilon} \tau_0, \quad \text{where } \tau_0 = O(1).$$

- The interface position is given by

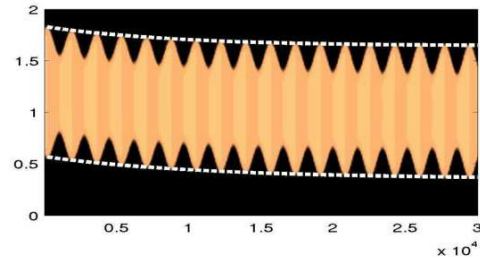
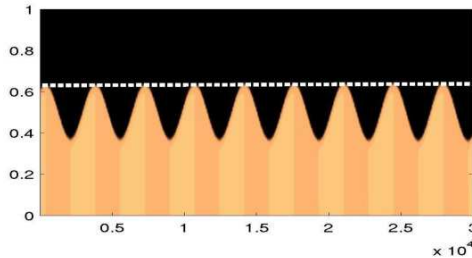
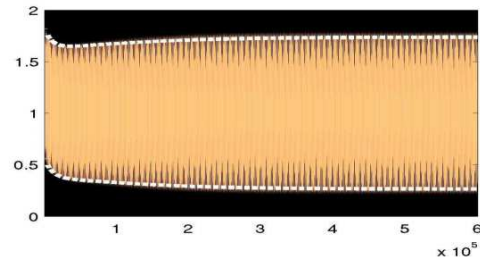
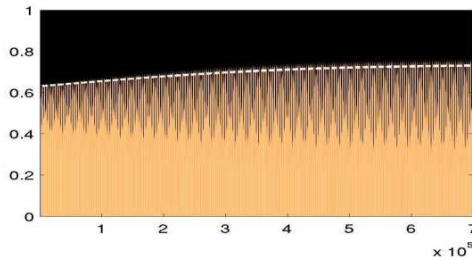
$$l(t) \sim l_0 + A(t) \cos(\sqrt{3/\tau_0 \varepsilon} D^{-1/2} t + \phi_0)$$

where A is the oscillation envelope that satisfies

$$\frac{D dA}{\varepsilon dt} = \left(\frac{1}{4}(1 - 3\beta^2) - \frac{1}{8\tau_0} \right) A - \frac{3}{4} A^3.$$

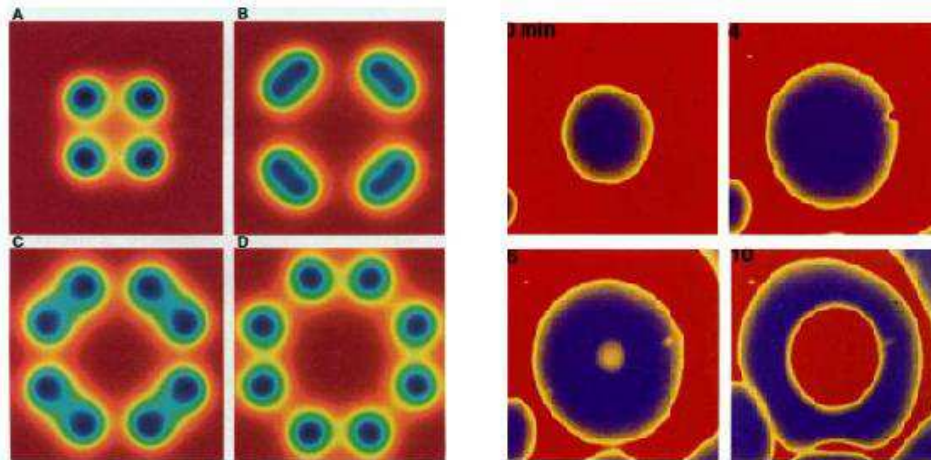
- Hopf bifurcation occurs when

$$\tau_{0h} = \begin{cases} \frac{1}{2(1-3\beta^2)} & \text{if } |\beta| < 3^{-1/2}; \\ \infty & \text{otherwise} \end{cases}.$$



Self-replication

- In 1993, Pearson reported self-replicating spots in the Gray-Scott model [J.E. Pearson, Science, 261, 189 (1993)].
- Experiments using Ferrocyanide-iodate-sulphite reaction (which GS models) confirmed numerical observation [Lee et.al, Nature, 1994].



Pearson (1993, numerics)

Lee et.al. (1994, lab)

- Self-replication was found in many other models, including chemical reactions, material science and nonlinear optics.

Gray-scott model

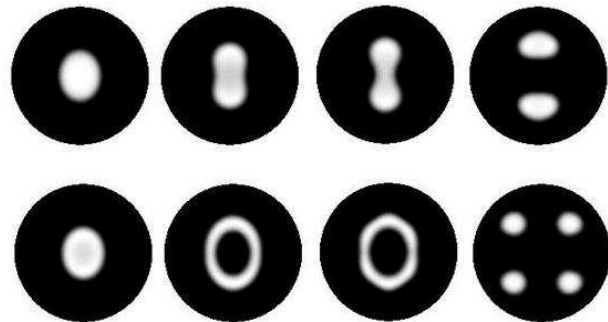
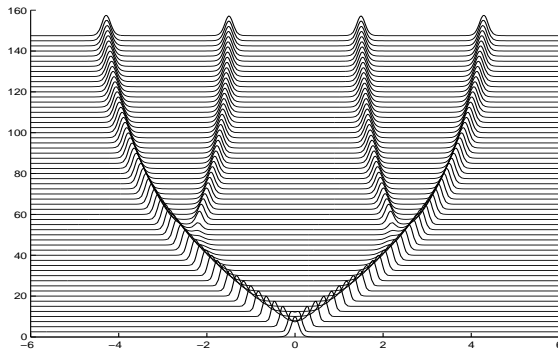
- Models a chemical reaction
- Large literature starting from 1990's: Doelman, Kaper, Muratov, Nishiura....

$$\begin{cases} u_t = D_v \Delta u - (F + k)u + vu^2 \\ v_t = D_u \Delta v + F(1 - v) + vu^2 \end{cases}$$

- Self-replication reduces to study a **fully-coupled 4-th order ODE:**

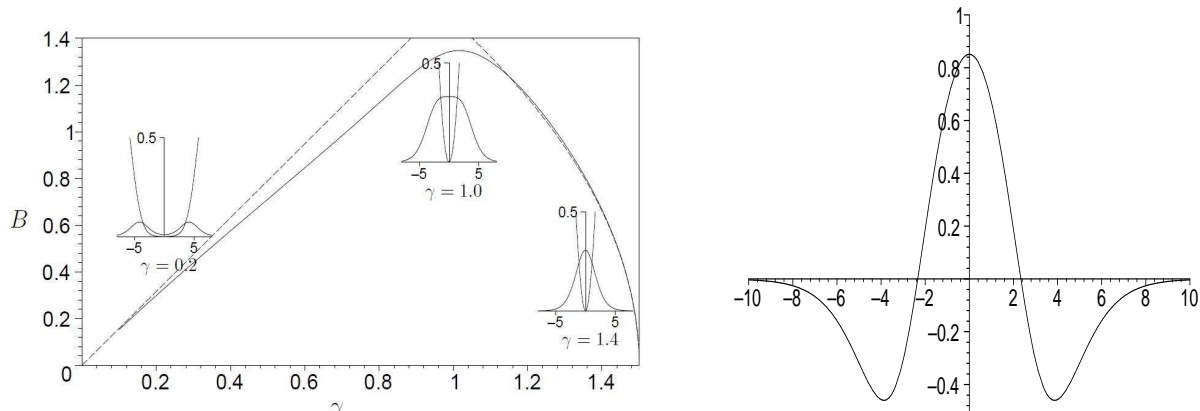
$$\begin{cases} \Delta U - U + U^2 V = 0 \\ \Delta V - U^2 V = 0 \\ V'(0) = 0 = U'(0), \quad V'(\infty) = B \end{cases}$$

- Replication has been observed in 1D and 2D (two different types):



Criteria for self-replication

- Four criteria, proposed by Nishiura and Ueyema (1999):
 1. The disappearance of the ground-state solution due to a fold point.
 2. The existence of a **dimple eigenfunction** at the fold point, responsible for the initiation of the self-replication process.
 3. Stability of the steady-state solution on one side of the fold point.
 4. The alignment (or cascade) of the fold points for K spots.
- Verification of these conditions is usually done numerically
- Analytic verification is an open problem for the GS model; order too high.



Simpler self-replication model in \mathbb{R}^N

$$u_t = \Delta u - u + \frac{(1 + a|x|^q) u^p}{\int_{\mathbb{R}^N} (1 + a|x|^q) u^{p+1}}; \quad \nabla u(0, t) = 0 \quad (5)$$

- Steady state satisfies (after rescaling):

$$0 = u_{rr} + \frac{N-1}{r} u_r - u + (1 + ar^q) u^p; \quad u'(0) = 0, \quad u > 0 \quad (\text{ss})$$

- Existence of ground state depends on a, q, p
- **Main result:** Self-replication occurs if a is gradually increased from 0, provided that

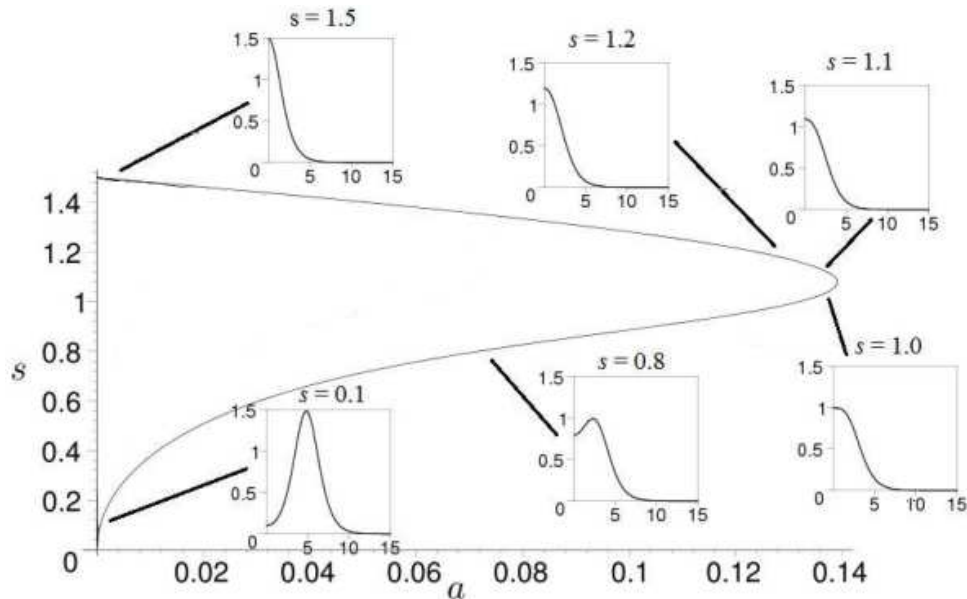
$$p > 1 \text{ and } q > \frac{(p-1)N}{2} \text{ if } N = 1 \text{ or } 2$$
$$1 < p < \frac{N+2}{N-2} \text{ and } q > \frac{(p-1)(N-1)}{2} \text{ if } N \geq 3.$$

Example: Bifurcation structure in 1-D

$$0 = u_{rr} - u + (1 + ar^2) u^2; \quad u'(0) = 0, \quad u > 0$$

- Two-bump solution connects to one-bump solution in a fold-point bifurcation. This is the **first condition for self replication**.

$$s := u(0; a)$$



Bifurcation structure in 3D

$$0 = u_{rrr} + \frac{2}{r}u_r - u + (1 + ar^q)u^2; \quad u'(0) = 0, \quad u > 0$$

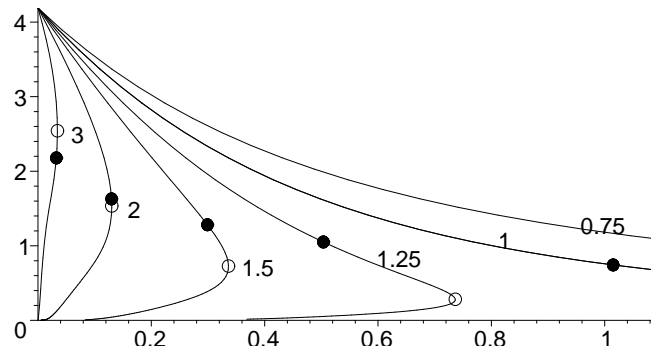
- If $q > 1$, there is a solution with $a \ll 1$, $u(0) \ll 1$ given by

$$u(r) \sim Cw(r - r_0) \quad \text{where} \quad r_0 = \left(\frac{1}{a}\right)^{1/q} \left(\frac{1}{q-1}\right)^{1/q}$$

where $w'' - w + w^p = 0$ is a 1-D ground state, C some constant.

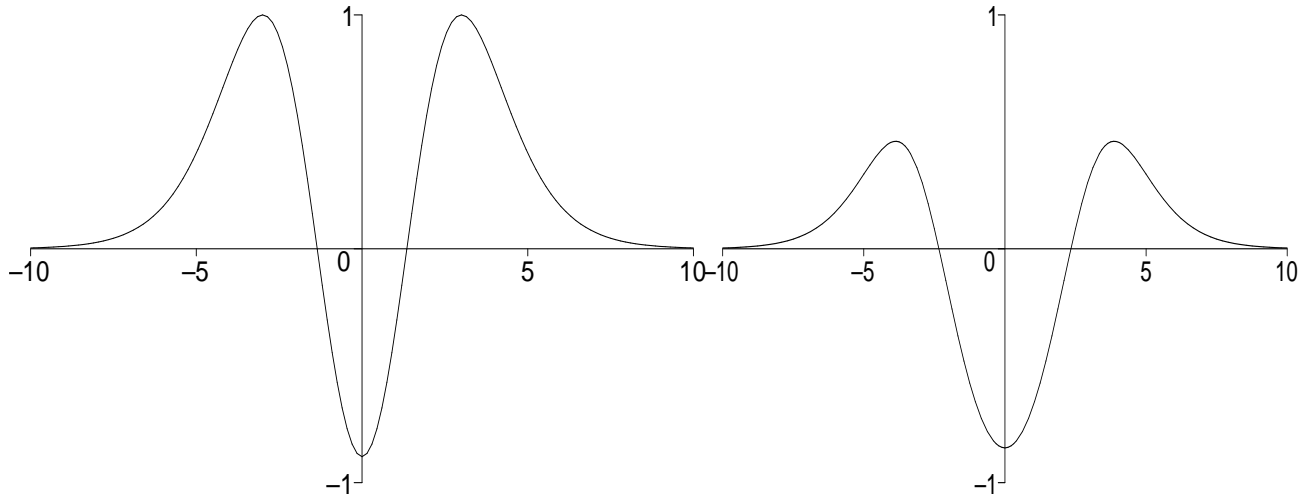
- If $q < 1$, there is a solution for $a \gg 1$ (no fold point)
- If $q = 1$, there is a solution with $a \gg 1$, $u(0) \ll 1$ given by

$$u(r) \sim Cw(r - r_0) \quad \text{where} \quad r_0 = O(\ln a)$$



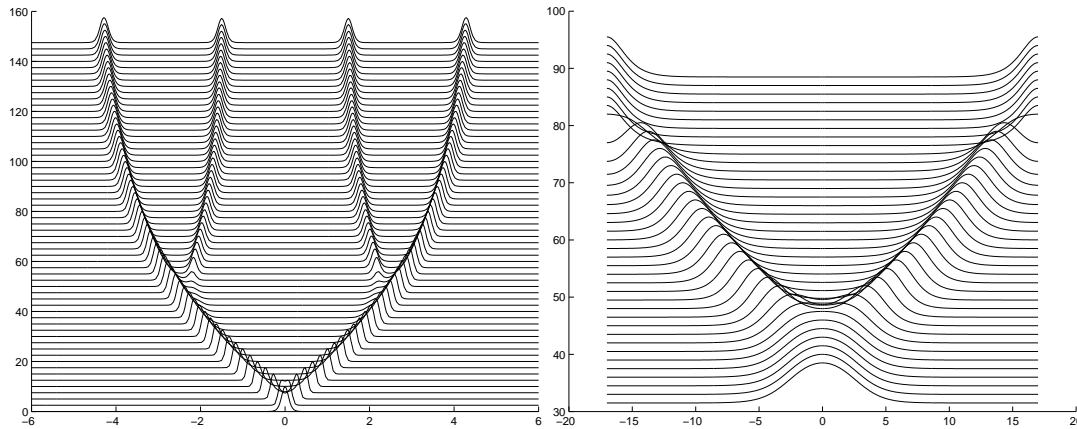
$p = 2$, q as indicated

- **Theorem:** There is a fold point when $q > 1$; no fold point if $q = 1$.
- **Theorem:** *The eigenfunction at the fold point has a dimple shape.* This verifies Nishiura-Ueyema condition 2



Dimple eigenvalue for simplified model (left) and for GS model (right)

Comparison with GS model



Left: GS model ([movie](#)). Right: Simplified model ([movie](#)).

- GS model: a cascade of self-replication events, resulting in multiple interior spikes.
- Simplified model: only one self-replication event; the spike moves to and merges with the boundary.
- Initial stages of self-replication mechanism are similar for the two models.

Nonradial stability ($N = 3$)

- Using spherical coordinates we decompose

$$Z(x, y, z) = \Phi(r)Y_l^m(\theta, \phi); \quad l = 0, 1, \dots; \quad m = 0, \pm 1 \dots \pm l$$

where Y_l^m are the spherical harmonics.

- For $l \geq 2$, The nonlocal term in (NLEP) disappears since $\int hZu^{p-1} = 0$, $l \geq 2$ and we get

$$\lambda_l \Phi = \Phi_{rr} + \frac{2}{r}\Phi_r - \frac{\gamma}{r^2}\Phi - \Phi + phu^{p-1}\Phi; \quad \gamma = l(l+1), \quad l \geq 2. \quad (\text{NREP})$$

- In the threshold case $q = p - 1$ and $a \gg 1$,

$$u(r) \sim Cw(r - r_0) \quad \text{where } r_0 = O(\ln a)$$

so that (NREP) becomes (LEP):

$$\lambda_l \Phi \sim \Phi_{rr} - \Phi + phu^{p-1}\Phi$$

which is **unstable!**

- Non-radial instability leads to **peanut-splitting**. [Click for movie](#)

Chemotaxis with Logistic growth

“Classical” chemotaxis model:

$$u_t = D_u u_{xx} - \chi (uv_x)_x, \quad v_t = D_v v_{xx} + \alpha u - \beta v. \quad (6)$$

- u is cell density, v is chemo-attractant.
- Models the ability of micro-organisms or cells to sense and move in response to chemical gradients.
- Introduced by Keller and Segel in 1970.
- Models:
 - Slime molds [Keller 1970],
 - Bacterial colonies [Hofer et.al 1995; Tyson Lubkin Murray 1999]
 - Skin patterns [Maini, Myerscough, Winters and Murray 1991; Murray and Myerscough, 1991]
 - Tumor formation [Owen, Markus, Sherratt, 1999]
- Mathematics:
 - Existence/uniqueness
 - Blowup analysis, asymptotics (“Chemotactic collapse)
 - Rich pattern formation
 - Reviews: Hillen 2009, Horstmann, 2003.

Chemotaxis with logistic self-production term

$$u_t = D_u u_{xx} - \chi (uv_x)_x + ru(1 - u/K), \quad v_t = D_v v_{xx} + \alpha u - \beta v. \quad (7)$$

- The logistic term ($r > 0$) prevents the chemotactic collapse
- Introduced in [Oster,Murray1989] and [Maini,Myerscough,Winters,Murray 1991].
- When $u(1 - u/K)$ is replaced by $u(1 - u)(u - a)$, solution consists of back-to-back interfaces whose stability was studied in detail by [Mimura,Tsujikawa,1996]
- For quadratic logistic terms, spike patterns are observed.
 - Complex spike dynamics were observed numerically by Hillen and his students [Hillen&Painter2001; Wang&Hillen2007]
 - **Movie:** Spike merging/emerging, oscillations, spatio-temporal chaos
 - “High-level” modelling by a particle dynamical system: [Hillen,Zielinski&Painter, 2013]

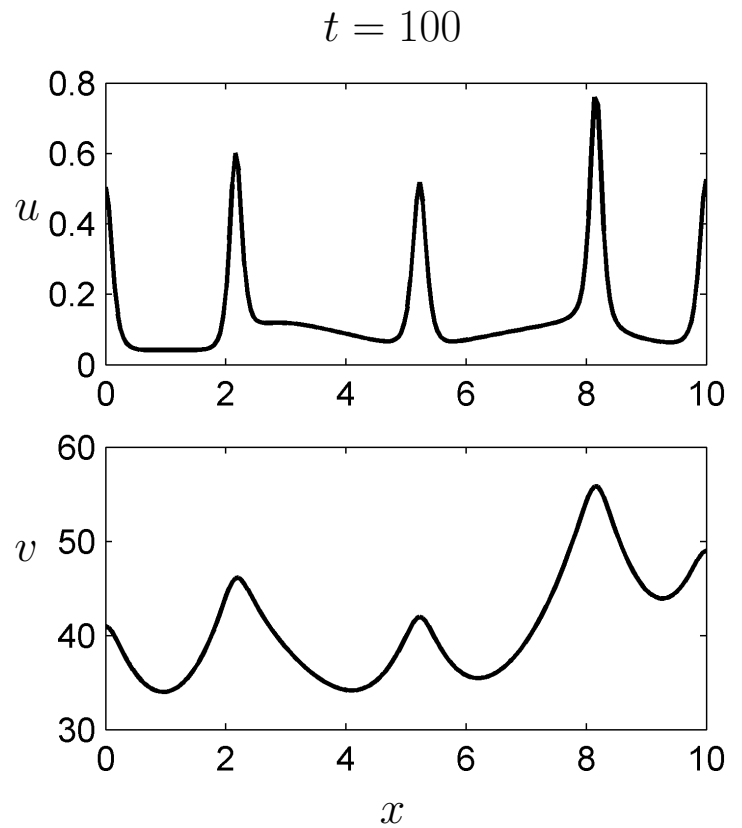
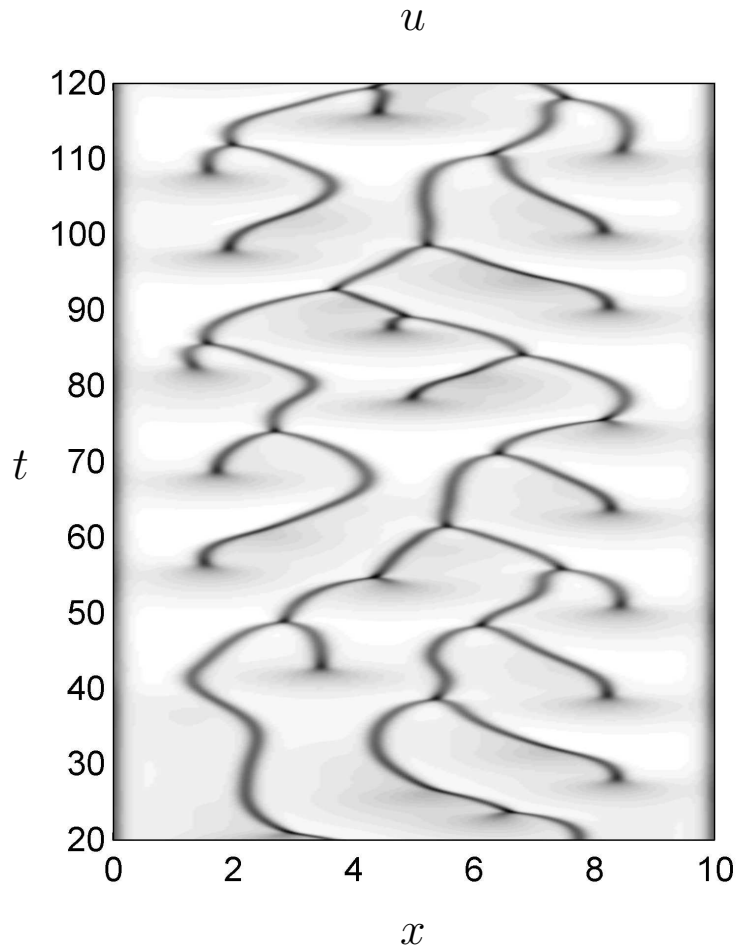


Figure 1: Left: numerical simulation of (8) on a domain of size 10 with $\varepsilon = 0.05$, $a = 15$. Contour plot of u in time and space is shown. Right: snapshot of the solution at $t = 100$. Software FlexPDE [?] was used for numerical simulations of the time-dependent system (8).

Basic mechanisms underlying spike dynamics

1. What is the profile of the spike?
2. Why/when do the spikes move towards each-other? **[Merging]**
3. What is the mechanism responsible for “spike insertion”? **[Emerging]**
4. Is it possible to stabilize an interior spike? [which is unstable for the “classical” KS model]

Regime 1: spike merging/emerging

- Rescale to this form:

$$u_t = (\varepsilon u_x - uv_x)_x + u - u^2, \quad \tau v_t = v_{xx} + \frac{a}{\varepsilon}u - v \quad (8)$$

$$u_x(\pm L, t) = 0 = v_x(\pm L, t) \quad (9)$$

- Biologically, this corresponds to small diffusion of cell density u (relative to the chemo-attractant v) and high chemo-attractant production by cells.

- Inner region:

$$x = \varepsilon y$$

$$u = U(y);$$

$$v = v_0 + \varepsilon W(y)$$

$$U_{0yy} - (U_0 W_{0y})_y = 0; \quad W_{0yy} + aU_0 = 0. \quad (10)$$

$$U_0 = \xi \operatorname{sech}^2 \left(y \sqrt{\frac{\xi a}{2}} \right); \quad W_{0y} = -\sqrt{2\xi a} \tanh \left(y \sqrt{\frac{\xi a}{2}} \right) \quad (11)$$

- Outer region: **two types.**

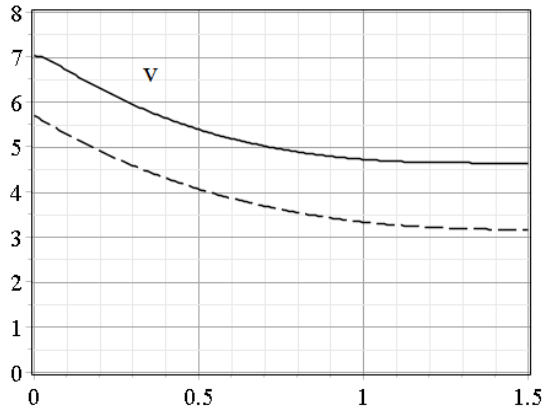
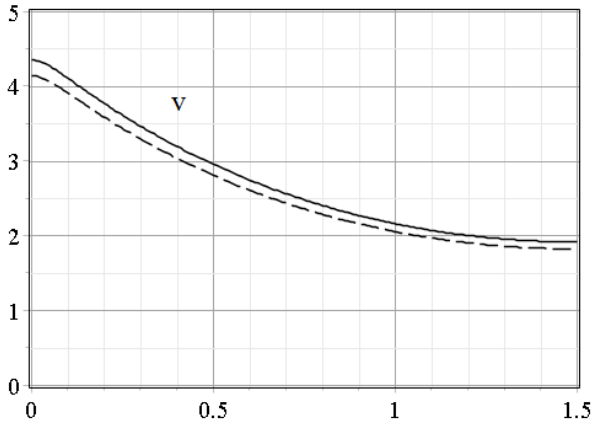
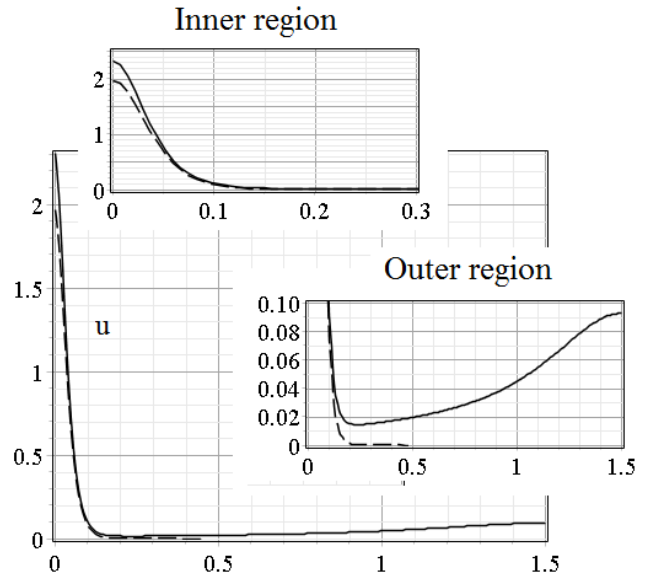
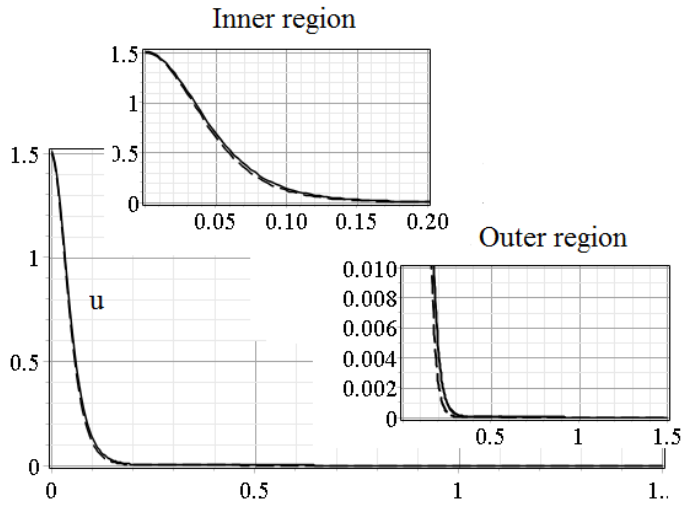
- Type 1:

$$\begin{aligned}v'' - v &= 0, \quad x \gg \varepsilon, \quad v'(L) = 0 \\v &= A \cosh(x - L), \quad x \gg \varepsilon.\end{aligned}\tag{12}$$

- Type 2: a novel, third order ODE for v :

$$(v - v'')(v'' - 1) + (v - v'')'v' = 0.\tag{13}$$

- The height ξ is determined using solvability condition to be $\xi = 3/2$ [for type 1]



Type I

Type II

Figure 2: Two types of steady state solutions to (ss). Parameter values are $\varepsilon = 0.1, L = 1.5$.

Merging behaviour (Type 1)

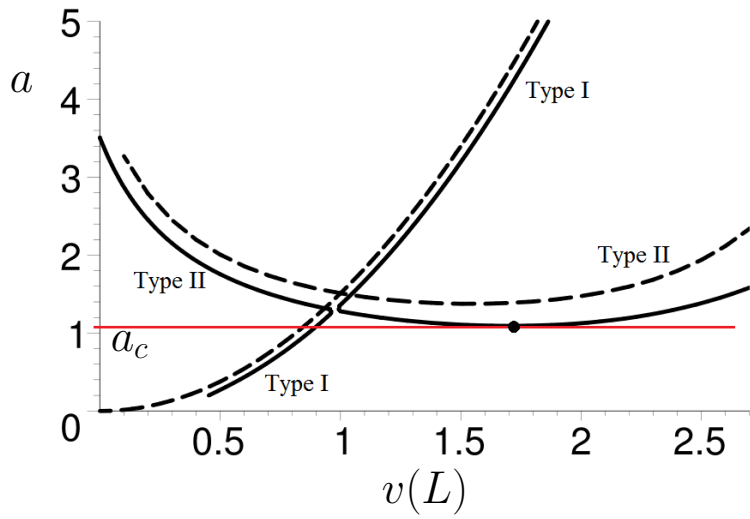
- A single interior spike is **structurally stable** (wrt to even perturbations) but **translationally unstable** (odd perturbation)
- **Main result:** there exists a **positive** translational eigenvalue λ given by

$$\lambda \frac{\sinh L \cosh(\mu L)}{\sqrt{2\xi a}} = \cosh L \cosh \mu L - \mu \sinh \mu L \sinh L; \quad \mu = \sqrt{1 + \lambda\tau}. \quad (14)$$

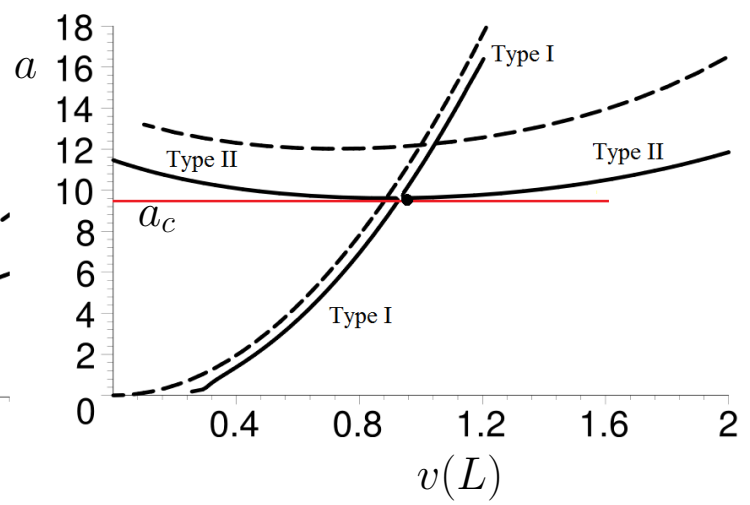
- Positivity follows from (14):
 - $lhs(14) \rightarrow \infty$ as $\lambda \rightarrow \infty$ and $rhs(14) \rightarrow -\infty$ as $\lambda \rightarrow \infty$.
 - When $\lambda = 0$ we have $lhs(14) = 0$ and $rhs(14) = 1$.
 - Thus there is a $\lambda > 0$ solution to (14).
- Conclusion: a single interior spike moves to the boundary of the interval.
- Corollary: two interior spikes will move either towards each other or to the boundary.

Emerging behaviour (Type 2)

- Due to a fold-point bifurcation in the *outer region*
- Corresponds to the disappearance of the solution to the 3rd order ODE.

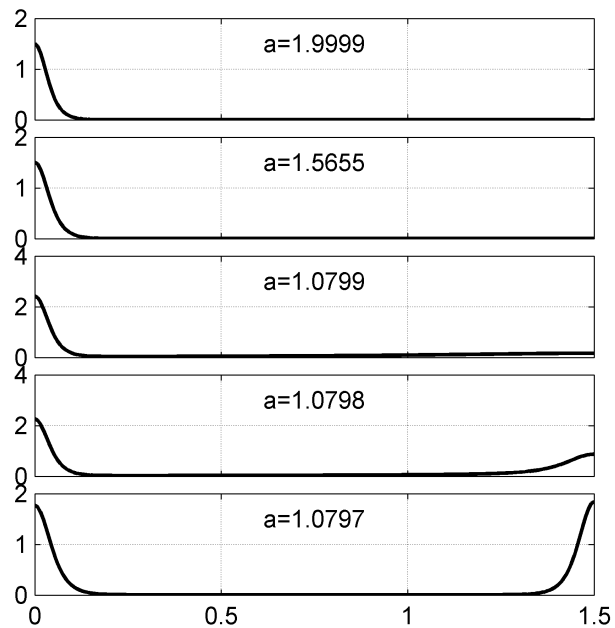


(a)

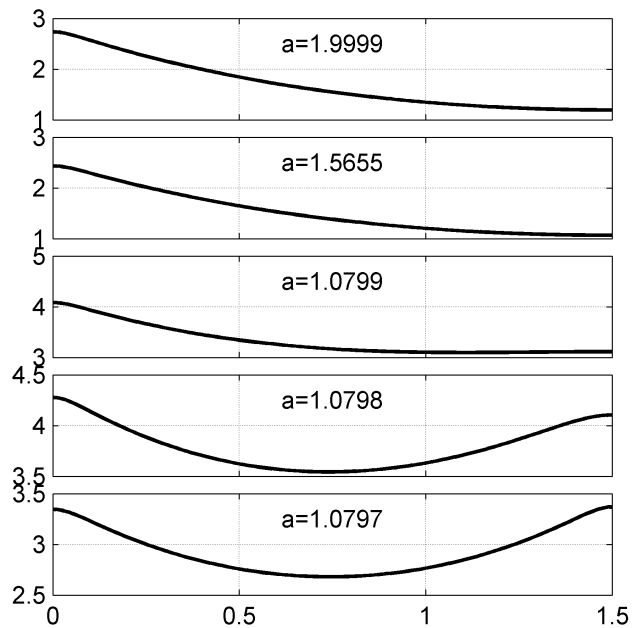


(b)

Figure 3: Bifurcation diagram for type I and II solutions. Solid curves denote the full problem whereas dotted curves are the asymptotics. The horizontal red line corresponds to the fold point a_c . (a) $\varepsilon = 0.05$, $L = 1.5$. (b) $\varepsilon = 0.15$, $L = 2.5$. Maple's boundary value problem solver and its continuation capabilities were used to compute the solid curves



u



v

Figure 4: Evolution of (8) with $\varepsilon = 0.05$, $L = 1.5$ and $a = 2 - 10^{-4}t$. Due to the fold point bifurcation, spike insertion occurs as a is decreased below $a_c \sim 1.08$. FlexPDE [?] was used for numerical computations

NEW: Stable interior spike

- Regime 2:

$$u_t = u_{xx} - (uv_x)_x + u - u^2, \quad \tau v_t = \varepsilon^2 v_{xx} - a\varepsilon v + u, \quad x \in [-L, L] \quad (15)$$

- Steady state: **triple-deck boundary layer:**

Inner layer: $x = \varepsilon y$

Middle layer: $x = \varepsilon^{1/2} z$

Outer layer: $x = x$

- Inner layer: as before,

$$u \sim \xi \operatorname{sech}^2 \left(y \sqrt{\frac{\xi a}{2}} \right), \quad v \sim \ln(u)$$

- Middle layer:

$$v \sim Ae^{-z}, \quad u \sim 4\xi \exp(Ae^{-z} - A), \quad A = \sqrt{\frac{2\xi}{a\varepsilon}}$$

- Outer layer: $u_{xx} + u \sim 0$,

$$u \sim B \cos(x - L), \quad B = \frac{4\xi}{\cos L} \exp\left(-\sqrt{\frac{2\xi}{a\varepsilon}}\right)$$

- Matching through the three layers, we get

$$v(L) \sim \frac{6}{\varepsilon a \cos L} \exp\left(-\sqrt{\frac{3}{a\varepsilon}}\right) + \sqrt{\frac{6}{a\varepsilon}} 2 \exp\left(-L\sqrt{\frac{a}{\varepsilon}}\right). \quad (16)$$

- The first term is dominant if $L > \frac{\sqrt{3}}{a}$ and second term is dominant if $L < \sqrt{3}/a$
- $v(L)$ has a minimum when $L = \sqrt{3}/a$.
- **THEOREM:** A single interior spike in regime 2 is **stable** if $L > \sqrt{3}/a$, it is **unstable** if $L < \sqrt{3}/a$.
- This is the first time that a interior **stable** spike was shown to exist for KS-type model!

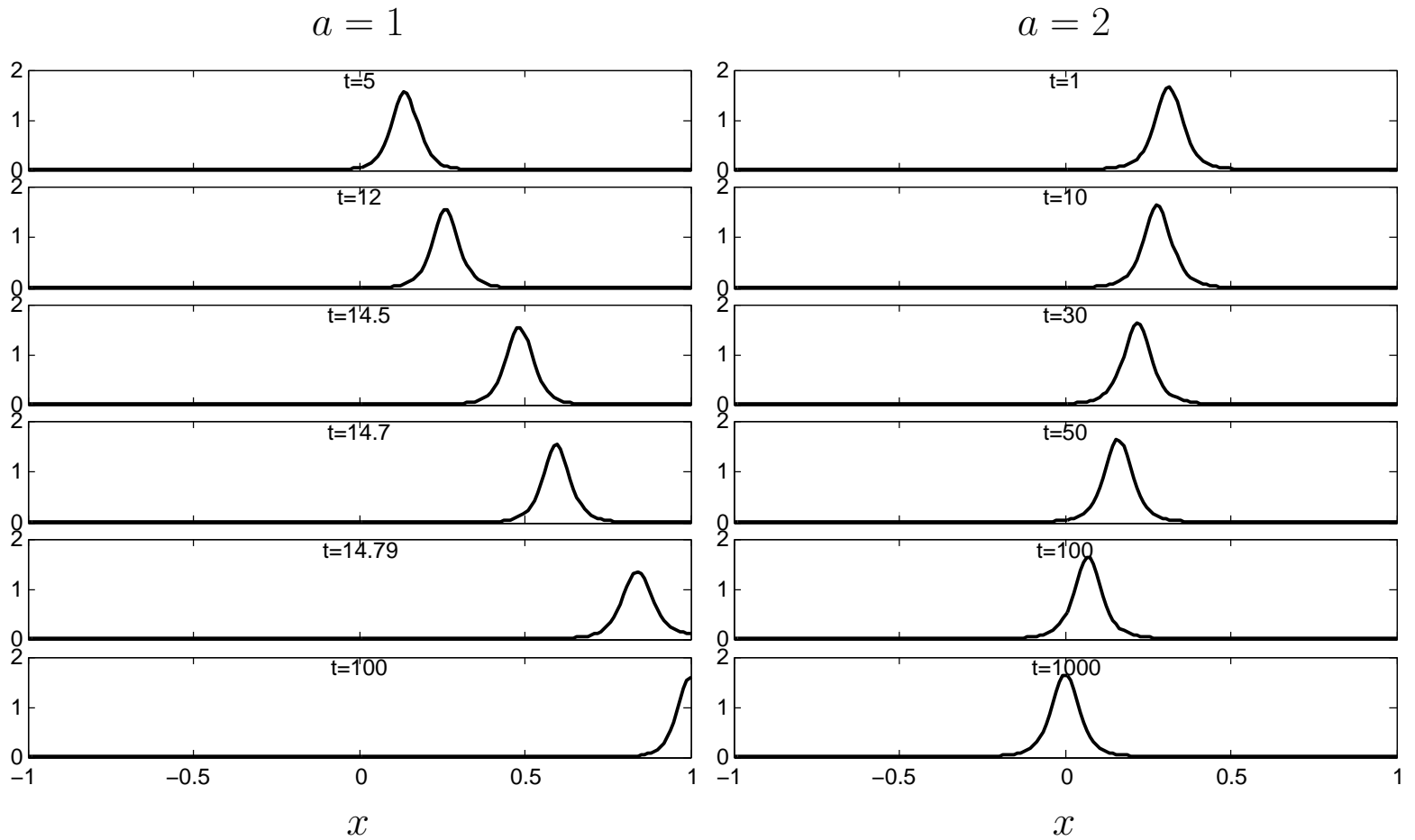


Figure 5: Numerical simulation of (15) with $\varepsilon = 0.05$, $\tau = 1$. Left: $a = 1$, the interior spike is unstable and moves to the boundary. Right: $a = 2$, the interior spike is stable. FlexPDE [?] was used for numerical computations.

Reference

T. Kolokolnikov, J Wei, and A. Alcolado, (2013) *Basic mechanisms driving complex spike dynamics in a chemotaxis model with logistic growth*, SIAM J.Appl.Math, 2014.

UCLA Model of hot-spots in crime

- Originally proposed by Short, D'Orsogna, Pasour, Tita, Brantingham, Bertozzi, and Chayes, 2008 [The UCLA model]
- Crime is ubiquitous but not uniformly distributed
 - Some neighbourhoods are worse than others, leading to crime "hot spots"
 - Crime hotspots can persist for long time.



Fig. 1. Dynamic changes in residential burglary hotspots for two consecutive three-month periods beginning June 2001 in Long Beach, CA. These density maps were created using ArcGIS.

Figure taken from Short et.al., *A statistical model of criminal behaviour*, 2008.

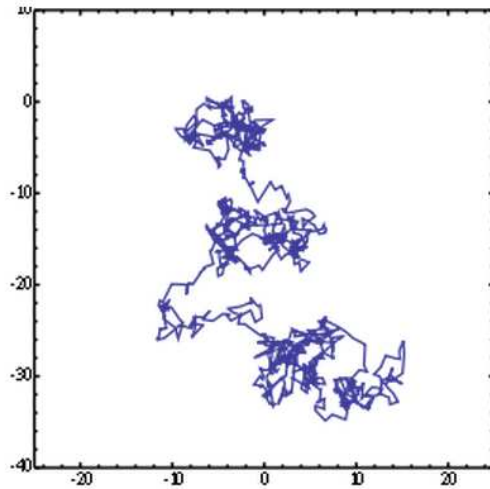
- Crime is temporaly correlated:
 - Criminals often return to the spot of previous crime
 - If a home was broken into in the past, the likelyhood of subsequent breakin increases
 - Example: graffitti "tagging"

Modelling criminal's movement

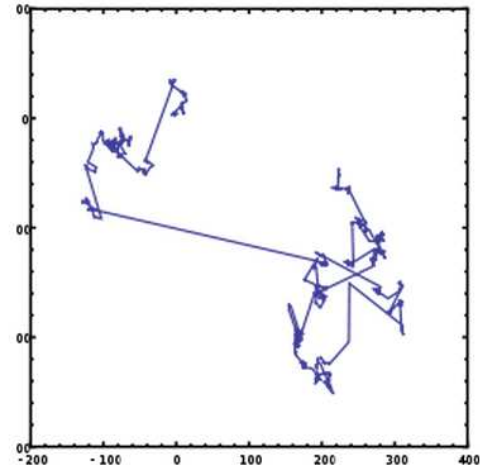
- In the original model, biased Brownian motion was used to model criminal's movement
- Our goal is to extend this model to incorporate more realistic motion
- Typical human motion consists short periods of fast movement [car trips] interspersed with long periods of slow motion [pacing, thinking about theorems, sleeping...]
- Such motion is often modelled using **Levi Flights**: At each time, the speed is chosen according to a **power-law distribution**; direction chosen at random: $|y(t + \delta t) - y(t)| = \delta t X$ where X is a power-law distribution whose distribution function is

$$f(d) = C |d|^{-\mu}$$

- μ is the power law exponent
 - In 1D, $1 < \mu \leq 3$; in 2D, $1 < \mu \leq 4$.
 - $\mu = 3$ corresponds to Brownian motion in one dimension.



Brownian motion



Levi flight motion

- González, Hidalgo, Barabási, *Understanding individual human mobility patterns*, *Nature* 2008, use cellphone data to suggest that human motion follows “truncated” Levi flight distribution with $\mu \approx 2.75$.

Discrete (cellular automata) model

- Two variables

$A_k(t) \equiv$ attractiveness at node k , time t ;

$N_k(t) \equiv$ criminal density at node k

- **Modelling attractiveness:** Attractiveness has static and dynamic component:

$$A_k(t) \equiv A^0 + B_k(t).$$

$$B_k(t + \delta t) = \underbrace{\left[(1 - \hat{\eta}) B_k(t) + \frac{\hat{\eta}}{2} (B_{k-1} + B_{k+1}) \right]}_{\text{"broken window effect"}} \underbrace{(1 - w\delta t)}_{\text{decay rate}} + \underbrace{\delta t A_k N_k \theta}_{\text{\# of robberies}}.$$

- $0 < \hat{\eta} < 1$ is the strength of broken window effect
- w is the decay rate

- **Modelling criminal movement:** Define the *relative weight* of a criminal moving from node i to node k , where $i \neq k$, as

$$w_{i \rightarrow k} = \frac{A_k}{l^\mu |i - k|^\mu}. \quad (17)$$

- l is the grid spacing, μ the Levi flight power law exponent
- The weight is *biased* by attractiveness field
- The *transition probability* of a criminal moving from point i to point k , where $i \neq k$, is

$$q_{i \rightarrow k} = \frac{w_{i \rightarrow k}}{\sum_{j \in \mathbb{Z}, j \neq i} w_{i \rightarrow j}}. \quad (18)$$

- Update rule for criminal density:

$$N_k(t + \delta t) = \sum_{i \in \mathbb{Z}, i \neq k} N_i \cdot (1 - A_i \delta t) \cdot q_{i \rightarrow k} + \Gamma \delta t. \quad (19)$$

- $A_i \delta t \equiv$ probability that criminal robs
- $(1 - A_i \delta t) \equiv$ probability that no robbery occurs
- $N_i \cdot (1 - A_i \delta t) \equiv$ expected number of criminals at node i that don't rob
- $N_i \cdot (1 - A_i \delta t) \cdot q_{i \rightarrow k} \equiv$ expected number of criminals that move from mode i to mode k .
- $\Gamma \delta t \equiv$ constant "feed rate" of the criminals

Take a limit $l, \delta t \ll 1$:

- Main trick is to write $A_i \sim A(x)$ where $x = li$; then

$$\begin{aligned}
 \sum_{j \in \mathbb{Z}, j \neq i} w_{i \rightarrow j} &= \sum_{j \in \mathbb{Z}, j \neq i} \frac{A_j}{l^\mu |i - j|^\mu} \\
 &= \sum_{j \in \mathbb{Z}, j \neq i} \frac{A_j - A_i}{l^\mu |i - j|^\mu} + \sum_{j \in \mathbb{Z}, j \neq i} \frac{A_i}{l^\mu |i - j|^\mu} \\
 &\sim \frac{1}{l} \int_{-\infty}^{\infty} \frac{A(y) - A(x)}{|x - y|^\mu} dy + l^{-\mu} 2\zeta(\mu) A(x)
 \end{aligned} \tag{20}$$

- We recognize the integral as ***fractional Laplacian***,

$$\Delta^s f(x) = 2^{2s} \frac{\Gamma(s + 1/2)}{\pi^{1/2} |\Gamma(-s)|} \int_{-\infty}^{\infty} \frac{f(x) - f(y)}{|x - y|^{2s+1}} dy, \quad 0 < s \leq 1.$$

- Key properties:

- The normalization constant is chosen so that the Fourier transform is:

$$\mathcal{F}_{x \rightarrow q} \{ \Delta^s f(x) \} = -|q|^{2s} \mathcal{F}_{x \rightarrow q} \{ f(x) \}. \tag{21}$$

- $s = 1$ corresponds to the usual Laplacian: $\Delta^s f(x) = f_{xx}$ if $s = 1$.

Continuum model

The continuum limit of CA model becomes

$$\frac{\partial A}{\partial t} = \eta A_{xx} - A + \alpha + A\rho. \quad (22)$$

$$\frac{\partial \rho}{\partial t} = D \left[A \Delta^s \left(\frac{\rho}{A} \right) - \frac{\rho}{A} \Delta^s (A) \right] - A\rho + \beta \quad (23)$$

where

$$s = \frac{\mu - 1}{2} \in (0, 1]; \quad \eta = \frac{l^2 \hat{\eta}}{2\delta t w}; \quad D = \frac{l^{2s} \pi^{1/2} 2^{-2s} |\Gamma(-s)|}{\delta t z \Gamma(2s + 1) w}; \quad \alpha = A_0/w; \quad \beta = \Gamma\theta/w^2.$$

- Separation of scales: if $l, \delta t \ll 1$ then

$$D\eta^{-s} \gg 1; \quad 0 < s \leq 1. \quad (24)$$

- The special case $s = 1$ ($\mu = 3$) corresponds to regular diffusion $\Delta^1 f(x) = f_{xx}$.

- We recover the UCLA model because:

$$A \left(\frac{\rho}{A} \right)_{xx} - \frac{\rho}{A} A_{xx} = \left(\rho_x - 2 \frac{\rho}{A} A_x \right)_x$$

- Note that $D \rightarrow \infty$ as $s \rightarrow 1^-$ since $|\Gamma(-s)| \sim 1/(1-s)$.

Simulation of continuum model

- Use a spectral method in space combined with method of lines in time.
- That is, we first discretize in space $x \in [0, L]$. To approximate $\Delta^s u$, we make use of Fourier transform:

$$\Delta^s u = \mathcal{F}^{-1} \left(-|q|^{2s} \mathcal{F}_{x \mapsto q} \{u\} \right). \quad (25)$$

- This becomes FFT on a bounded interval
- **Matlab code** to estimate the discretization of $\Delta^s u(x)$, $x \in [0, 1]$:

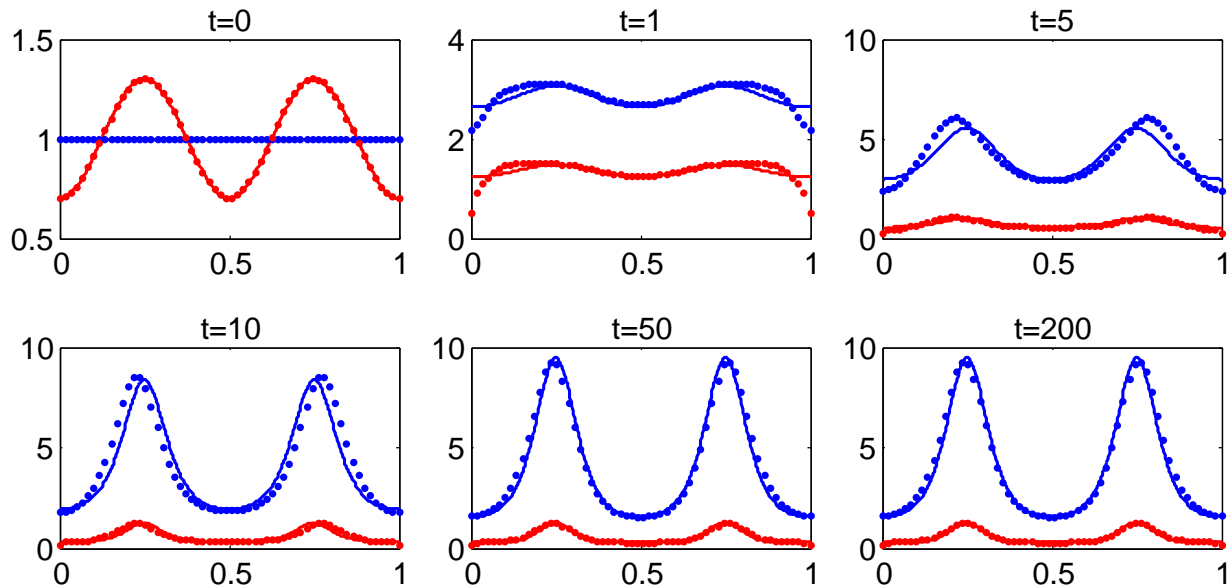
```
n = numel(u);  
q = 2*pi*[0:n/2-1, -n/2:-1]';  
LaplaceS_u = ifft(-q.^(2*s).*fft(u));
```

- This implicitly imposes periodic boundary conditions on the solution.

Comparison: discrete vs. continuum

Example: Take $\mu = 2.5$, $n = 60$, $l = 1/60$, $\hat{\eta} = 0.1$, $\delta t = 0.01$, $A_0 = 1$, $\Gamma = 3$.

Then the continuum model gives $s = 0.75$, $\eta = 0.001388$, $D = 0.1828$, $\alpha = 1$, $\beta = 3$.



Discrete model is represented by dots; continuum model by solid curves. Blue is A , red is ρ . Two hot-spots form.

Turing instability analysis

$$\frac{\partial A}{\partial t} = \eta A_{xx} - A + \alpha + A\rho, \quad \frac{\partial \rho}{\partial t} = D \left[A \Delta^s \left(\frac{\rho}{A} \right) - \frac{\rho}{A} \Delta^s (A) \right] - A\rho + \beta$$

Steady state:

$$\bar{A} = \alpha + \beta; \quad \bar{\rho} = \frac{\beta}{\alpha + \beta}.$$

Linearization:

$$A(x, t) = \bar{A} + \phi e^{\lambda t} e^{ikx}, \quad (26a)$$

$$\rho(x, t) = \bar{\rho} + \psi e^{\lambda t} e^{ikx}. \quad (26b)$$

Using the Fourier transform property, we have:

$$\Delta^s e^{ikx} = -|k|^{2s} e^{ikx}$$

so the eigenvalue problem becomes

$$\begin{bmatrix} -\eta|k|^2 - 1 + \bar{\rho} & \bar{A} \\ \frac{2\bar{\rho}}{A} D|k|^{2s} - \bar{\rho} & -D|k|^{2s} - \bar{A} \end{bmatrix} \begin{bmatrix} \phi \\ \psi \end{bmatrix} = \lambda \begin{bmatrix} \phi \\ \psi \end{bmatrix}. \quad (27)$$

The dispersion relationship is then given by

$$\lambda^2 - \tau\lambda + \delta = 0$$

where

$$\tau = -D|k|^{2s} - \eta|k|^2 - \bar{A} - 1 + \bar{\rho}; \quad \delta = D|k|^{2s} (\eta|k|^2 + 1 - 3\bar{\rho}) + \eta|k|^2 \bar{A} + \bar{A}.$$

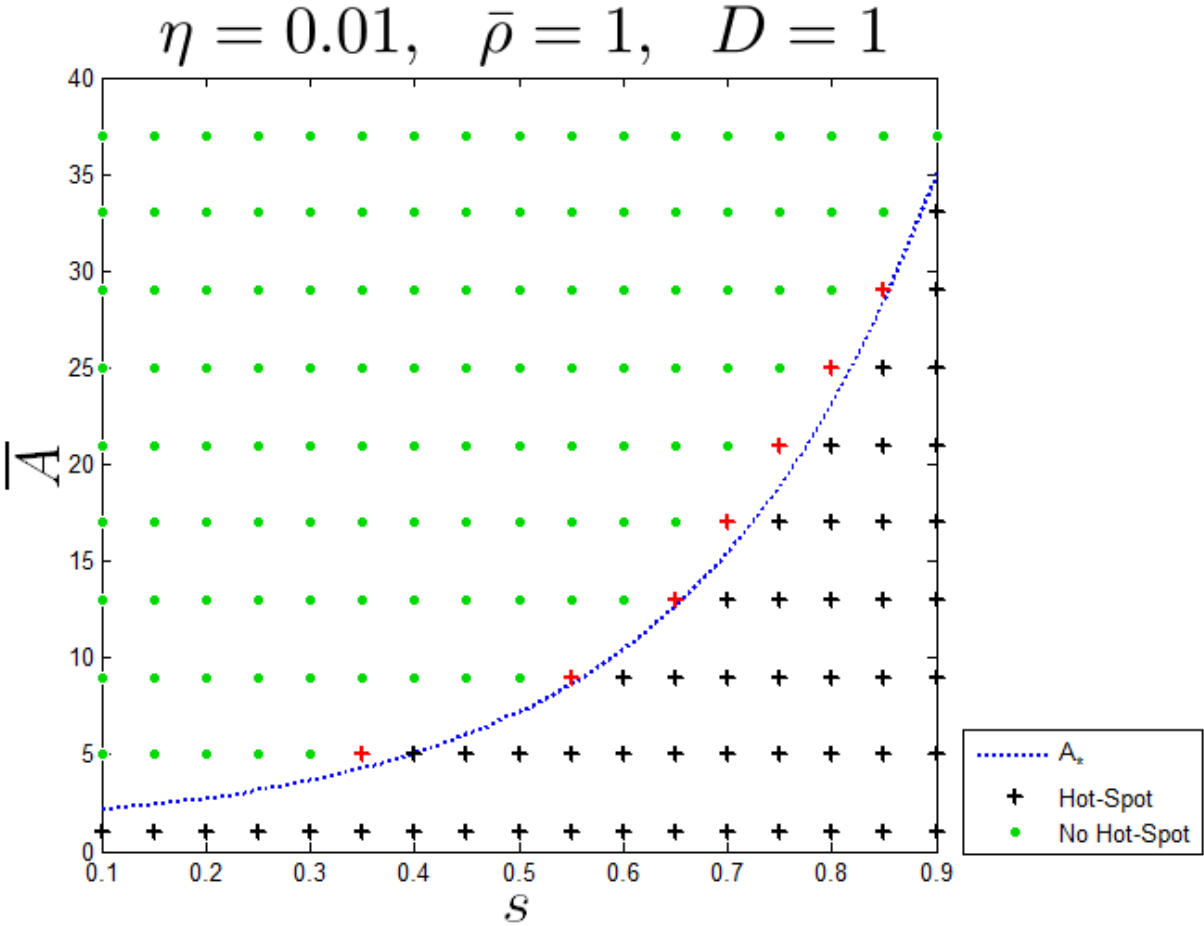
Note that $\tau < 0$ so the steady state is stable iff $\delta > 0$ **for all** k . Equilibrium is stable if $\bar{\rho} < 1/3$. If $\bar{\rho} > 1/3$ then equilibrium is unstable iff

$$\bar{A} < D\eta^s x^s \left(-1 + \frac{3\bar{\rho}}{x+1} \right) \quad (28)$$

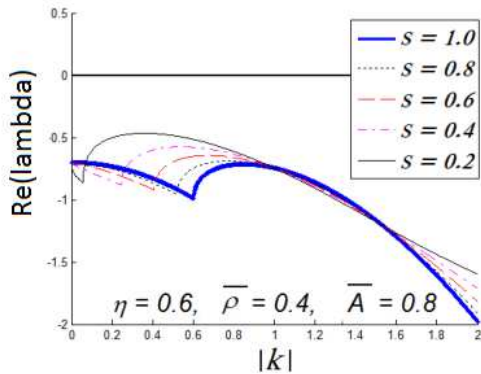
where x is the unique positive root of

$$x^2 + x(2 + 3\bar{\rho}(1-s)/s) + 1 - 3\bar{\rho} = 0.$$

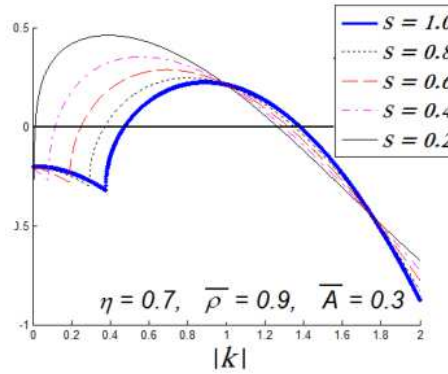
Comparison with numerics



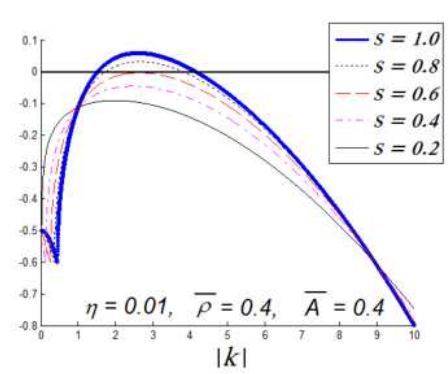
The effect of changing s on dispersion relationship



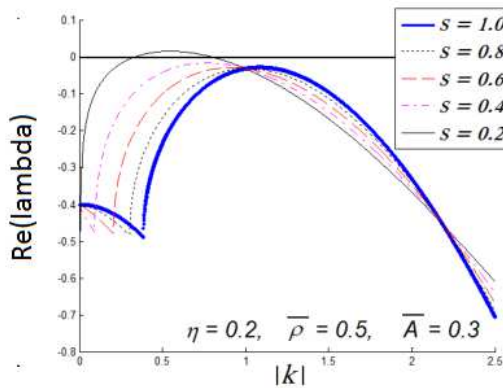
(a) A stable regime



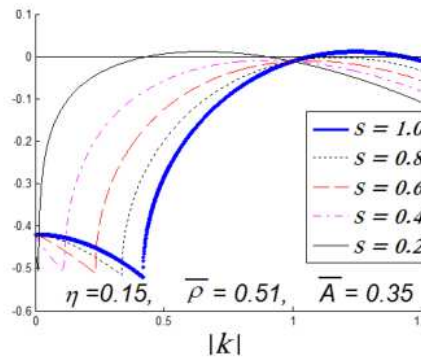
(b) An unstable regime



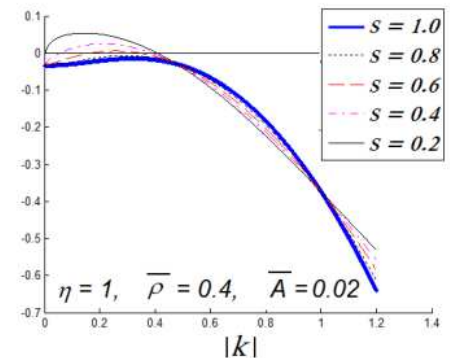
(c) Fractional diffusion leads to stability



(d) Fractional diffusion leads to instability



(e) Fractional diffusion leads to stability and then instability



(f) A regime in which $|k_2| < |k_1| = 1$

Dominant instability [biggest λ]

- Recall that in terms of original gridsize l and time step δt , we have:

$$s = \frac{\mu - 1}{2} \in (0, 1]; \quad \eta = \frac{l^2 \hat{\eta}}{2\delta t w}; \quad D = \frac{l^{2s} \pi^{1/2} 2^{-2s} |\Gamma(-s)|}{\delta t z \Gamma(2s + 1) w}$$

so that $\eta^{-s} D = O((1 - s)^{-1} (\delta t)^{s-1}) \gg 1$, $0 < s \leq 1$

- For a physically relevant regime, the continuum model satisfies the key relationship***

$$\boxed{\eta^{-s} D \gg 1.} \tag{29}$$

Change the variables $k = x^{1/2} \eta^{-1/2}$ and let $M = D \eta^{-s} \gg 1$. Then we obtain

$$\tau = -M x^s - x^2 + \bar{\rho} - 1 - \bar{A}; \quad \delta = M x^s (x + 1 - 3\bar{\rho}) + x \bar{A} + \bar{A}.$$

The fastest growing mode corresponds to the maximum of the dispersion curve:

$$\lambda^2 - \tau \lambda + \delta = 0 \quad \text{and} \quad \lambda = \tau_x / \delta_x.$$

- Asymptotically, this becomes

$$k_{\text{fastest}}(s) \sim \left[\frac{s\bar{\rho}(-2 + 3\bar{A} + 6\bar{\rho})}{D\eta} \right]^{\frac{1}{2(s+1)}}, \quad D\eta^{-s} \gg 1. \quad (30)$$

$$\text{Expected number of "bumps"} \approx \text{floor} \left(\frac{L}{2\pi} k_{\text{fastest}} \right). \quad (31)$$

- k_{fastest} is at a maximum when s satisfies

$$\log \left(\frac{\bar{\rho}(-2 + 3\bar{A} + 6\bar{\rho})}{D\eta} s \right) = s + 1$$

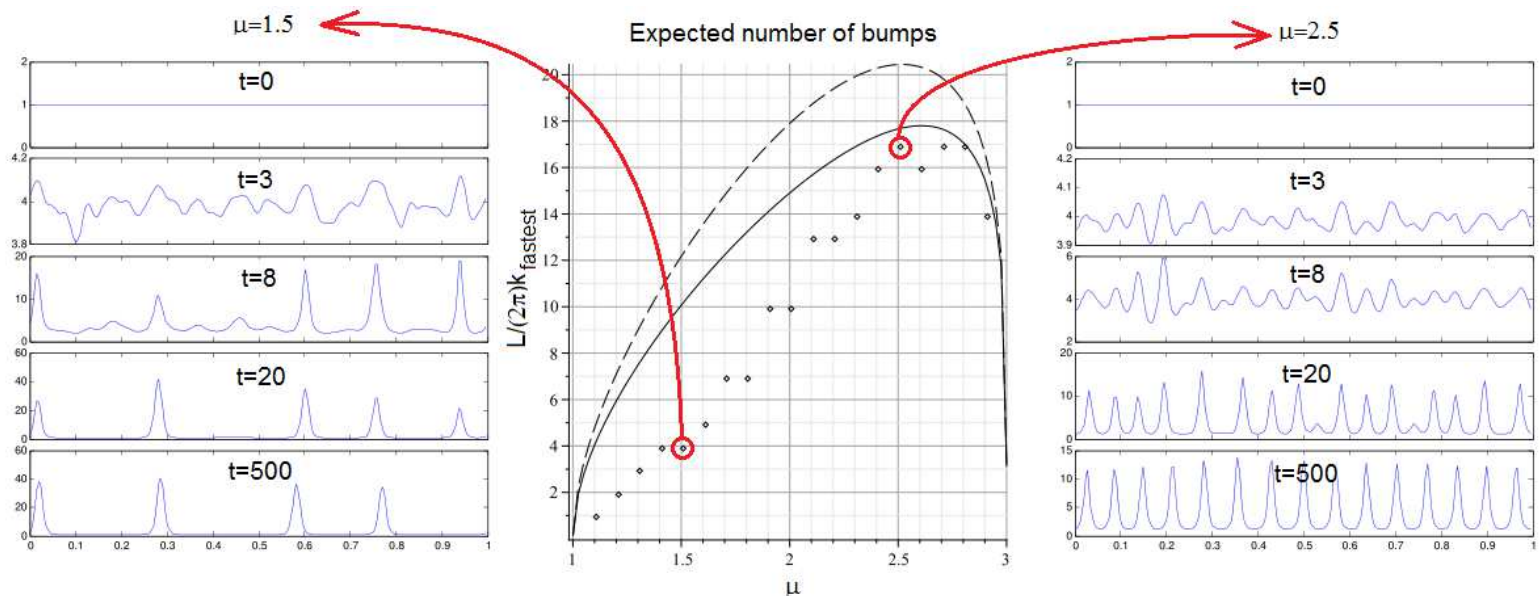
- In terms of original variables:

$$\mu_{\text{optimal}} \sim 3 - 2/\log(1/\delta t)$$

- Conclusion: the **optimal** exponent (from the point of view of criminals) is just below the Brownian motion $\mu = 3$

Comparison with numerics

$$l = 0.01, \delta t = 0.05, \hat{\eta} = 0.02, A_0 = 1, \Gamma = 3$$



- Intuitively, if the criminals move too fast or too sporadically (smaller μ), they will miss some opportunities for looting. On the other hand, they will also miss opportunities if they move very little (μ close to 3). The best strategy should therefore be a compromise between widely exploring the state space and exploring localized niches.

- The initial instability has sinusoidal shape
- Eventually, hot-spot forms.
 - Hot-spots are localized regions which are *not* of the sinusoidal shape!
 - In general, the total number of stable hot-spots *does not* correspond to fastest-growing Turing mode!
 - The hot-spot regime is separate from the Turing regime!

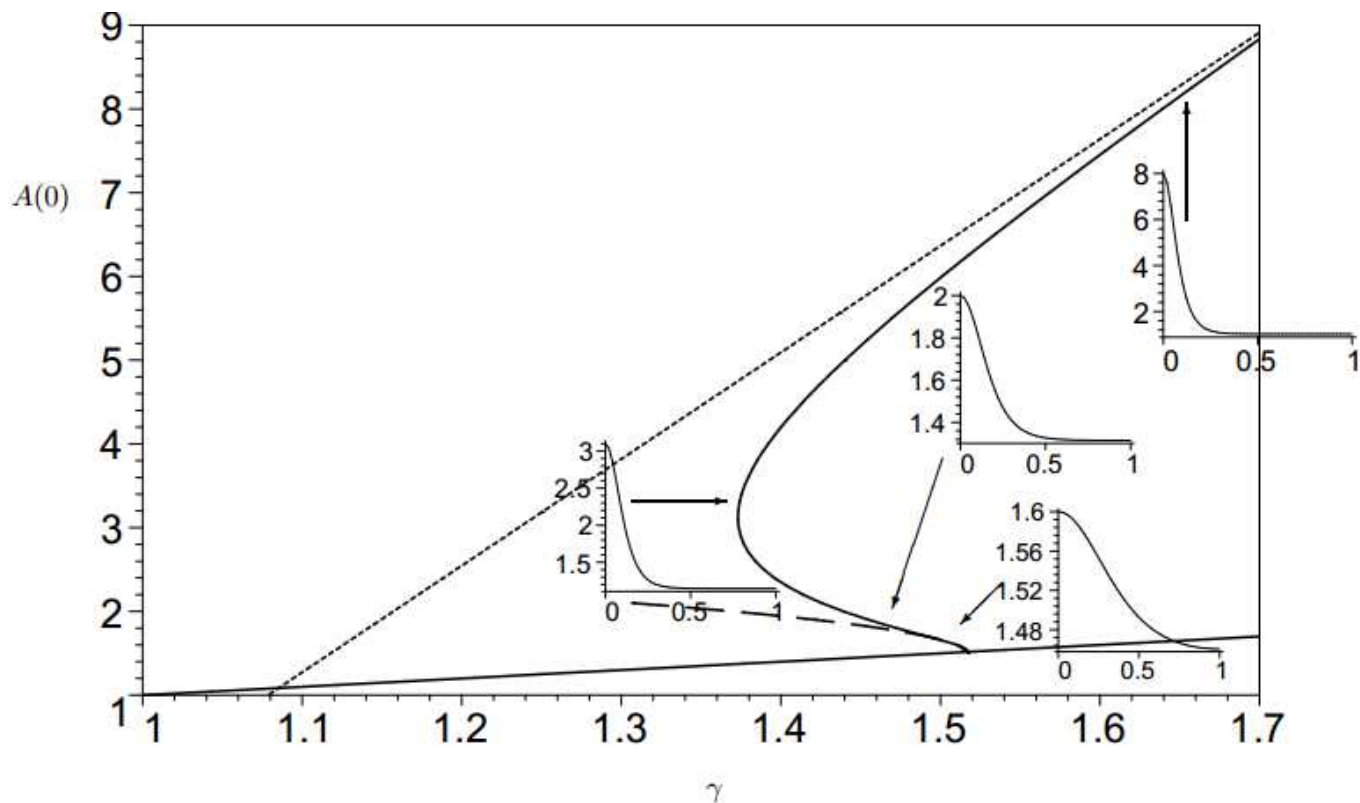


FIGURE 7. Numerically computed bifurcation diagram of $A(0)$ vs. γ . The parameter values are $\alpha = 1, \varepsilon = 0.05, x \in [0, 1]$, and $D = 2$. A localized hot-spot appears for large values of $A(0)$. The asymptotics $A(0) \sim \frac{2(\gamma - \alpha)}{\varepsilon\pi}$ (see (2.19)) are shown by a dotted line. The constant steady state $A \sim \gamma$ is indicated by a solid straight line. Turing patterns are born from the spatially uniform steady state as a result of a Turing bifurcation at $\gamma \sim 3\alpha/2 = 1.5$. The weakly nonlinear regime is indicated by a dashed parabola coming out of the bifurcation point. Inserts shows the change in the shape of the profile $A(x)$ along the bifurcation curve.

Construction of hotspot solution

Hotspot solution satisfies:

$$0 = \eta A_{xx} - A + \alpha + A\rho; \quad 0 = D \left[A\Delta^s \left(\frac{\rho}{A} \right) - \frac{\rho}{A} \Delta^s (A) \right] - A\rho + \beta \quad (32)$$

and is periodic on $[-1, 1]$.

- **Key transformation:** Let $\rho = vA^2$; then

$$0 = \eta A_{xx} - A + \alpha + A^3v; \quad 0 = D [A\Delta^s (vA) - vA\Delta^s (A)] - A^3v + \beta \quad (33)$$

- **Inner problem:** Change variables $x = \eta^{1/2}y$; then

$$0 = A_{yy} - A + \alpha + A^3v; \quad 0 = D\eta^{-s} [A\Delta^s (vA) - vA\Delta^s (A)] - A^3v + \beta$$

- As before, $D\eta^{-s} \gg 1$ so that in the inner region,

$$A\Delta_y^s (vA) - vA\Delta_y^s (A) \sim 0 \implies v(y) \sim \text{const.} \sim v_0$$

- Change variables $A = v_0^{-1/2}w(y)$, then

$$w_{yy} - w + w^3 = 0 \implies w = \sqrt{2} \operatorname{sech}(y)$$

- To determine v_0 , integrate (33) and use the identity $\int f \Delta^s g - g \Delta^s f = 0$; then

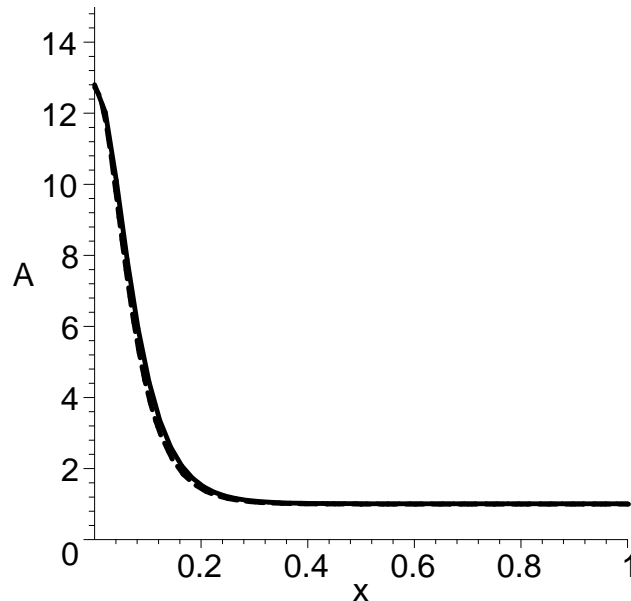
$$\int A^3 v_0 \sim \int \beta$$

- The final result is

$$A(x) \sim \begin{cases} A_{\max} w(x/\sqrt{\eta}), & x = O(\varepsilon) \\ \alpha, & x \gg O(\varepsilon). \end{cases}$$

$$A_{\max} \sim \frac{2l\beta\pi^{-3/2}}{\sqrt{\eta}}$$

where l is the half-width of the spot.



Stability of hot-spots (1D, $s = 1$)

- **Localized states:** Consider a periodic pattern consisting of **localized** hotspots of radius l . It is stable iff $l > l_c$ where

$$l_c := \frac{(\eta D)^{1/4} \pi^{1/2} \alpha^{1/2}}{\beta^{3/4}}.$$

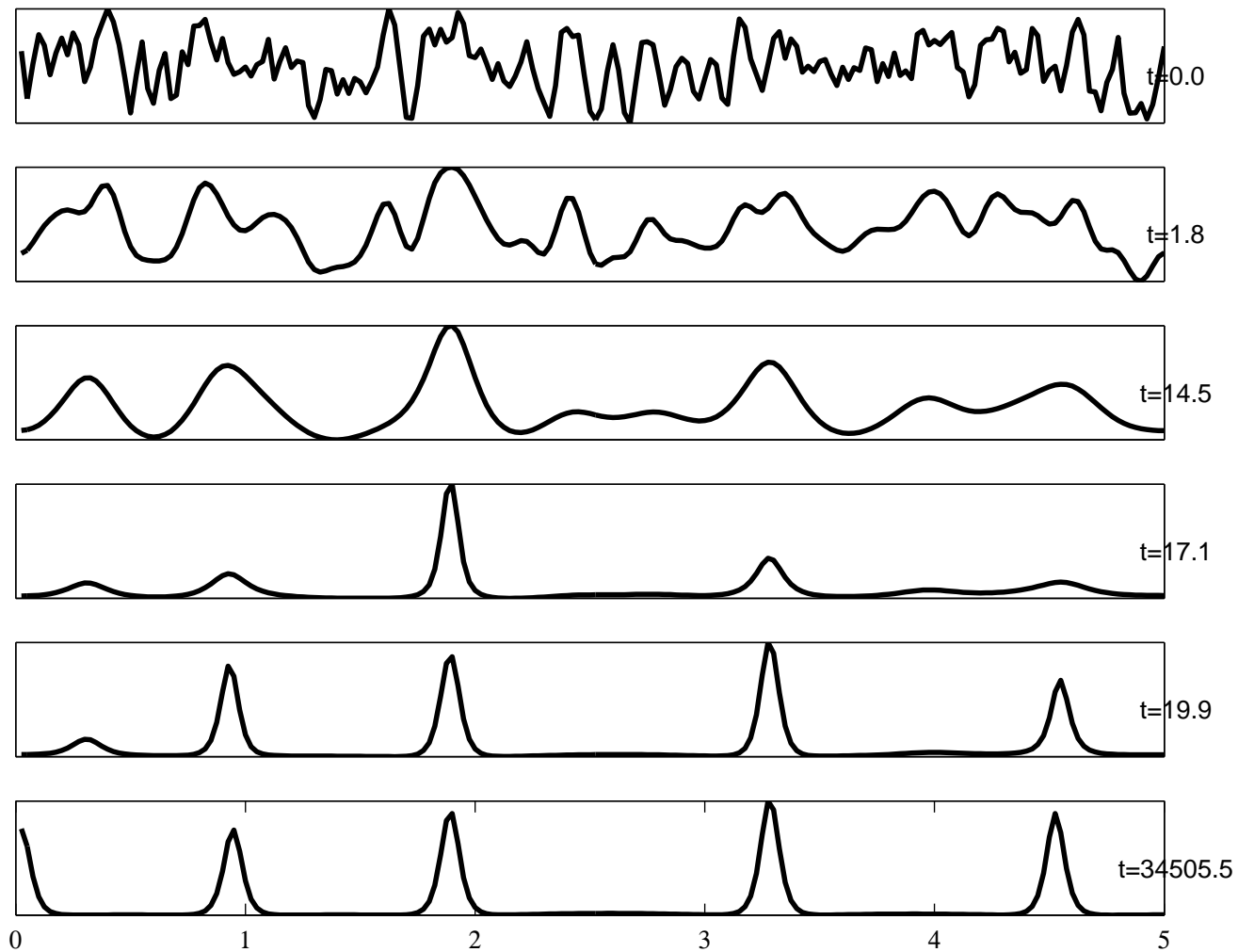
- **Turing instability in the limit $\varepsilon \rightarrow 0$:**

- Preferred Turing characteristic length:

$$l_{\text{turing}} \sim 2\pi \left[\frac{D\eta}{\bar{\rho}(-2 + 3\bar{A} + 6\bar{\rho})} \right]^{1/4}, \quad D\eta^{-1} \gg 1$$

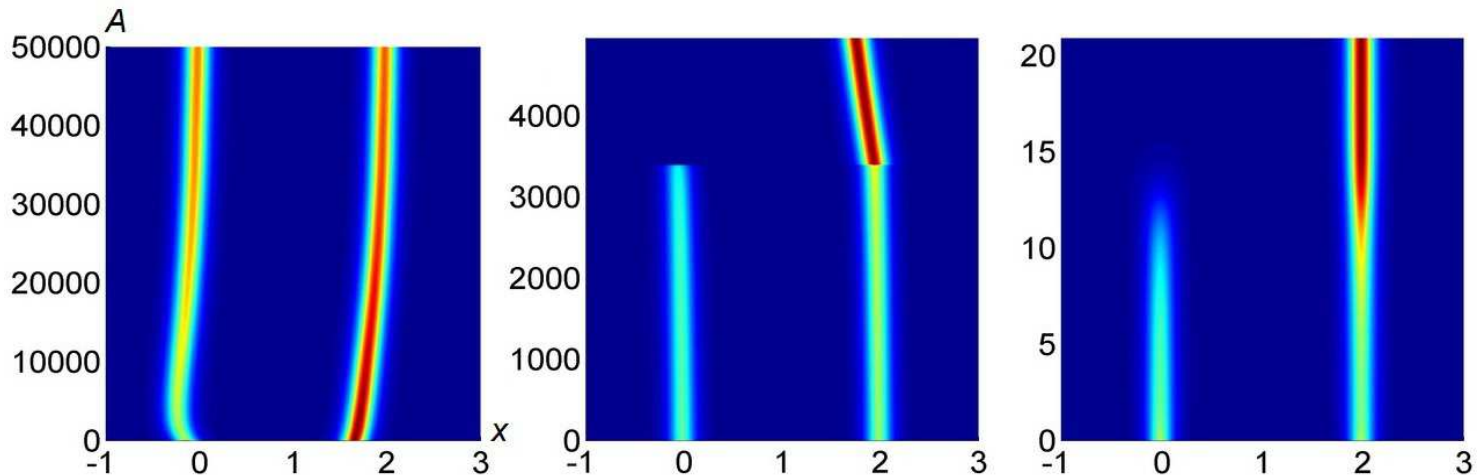
- Note that both $O(l_c) = O(l_{\text{turing}}) = O((D\eta)^{1/4})!$

Example: $l_c = 0.60$; $l_{turing} = 0.13 < l_c$



Small and large eigenvalues

- Near-translational invariance leads to “small eigenvalues (perturbation from zero)” corresponding eigenfunction is $\phi \sim w'$.
- Large eigenvalues are responsible for “competition instability”.
- Small eigenvalues become unstable before the large eigenvalues.
- Example: Take $l = 1, \gamma = 2, \alpha = 1, K = 2, \varepsilon = 0.07$. Then $D_{c,\text{small}} = 20.67, D_{c,\text{large}} = 41.33$.
 - if $D = 15 \implies$ two spikes are stable
 - if $D = 30 \implies$ two spikes have very slow developing instability
 - if $D = 50 \implies$ two spikes have very fast developing instability



Stability: large eigenvalues

- **Step 1:** Reduces to the nonlocal eigenvalue problem (NLEP):

$$\lambda\phi = \phi'' - \phi + 3w^2\phi - \chi \left(\int w^2\phi \right) w^3 \quad \text{where } w'' - w + w^3 = 0. \quad (34)$$

with

$$\chi \sim \frac{3}{\int_{-\infty}^{\infty} w^3 dy} \left(1 + \varepsilon^2 D \left(1 - \cos \frac{\pi k}{K} \right) \frac{\alpha^2 \pi^2}{4l^4 \beta^3} \right)^{-1}$$

- **Step 2: *Key identity*:** $L_0 w^2 = 3w^2$, where $L_0\phi := \phi'' - \phi + 3w^2\phi$. Multiply (34) by w^2 and integrate to get

$$\lambda = 3 - \chi \int w^5 = 3 - \chi \frac{3}{2} \int w^3$$

Conclusion: (34) is stable iff $\chi > \frac{2}{\int w^3} \iff D > D_{c,\text{large}}$.

- This NLEP in 1D can be fully solved!!

Stability: small eigenvalues

- Compute asymmetric spikes
- They bifurcate from symmetric branch
- The bifurcation point is precisely when $D = D_{c,\text{small}}$.
- This is “cheating”... but it gets the correct threshold!!

Stability of K spikes

- Possible boundary conditions:

Config type	Boundary conditions for ϕ
Single interior spike on $[-l, l]$ even eigenvalue	$\phi'(0) = 0 = \phi'(l)$
Single interior spike on $[-l, l]$ odd eigenvalue	$\phi(0) = 0 = \phi(l)$
Two half-spikes at $[0, l]$	$\phi'(0) = 0 = \phi(l)$
K spikes on $[-l, (2K - 1)l]$, Periodic BC	$\phi(l) = z\phi(-l), \quad \phi'(l) = z\phi'(-l),$ $z = \exp(2\pi ik/K), \quad k = 0 \dots K - 1$
K spikes on $[-l, (2K - 1)l]$, Neumann BC	$\phi(l) = z\phi(-l), \quad \phi'(l) = z\phi'(-l),$ $z = \exp(\pi ik/K), \quad k = 0 \dots K - 1$

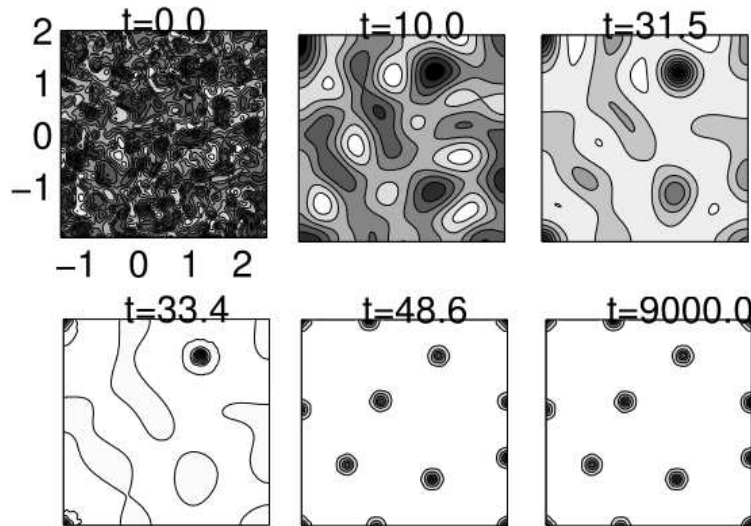
(same BC for ψ)

Two dimensions

Given domain of size S , let

$$K_c := 0.07037\eta^{-3/8}D^{-1/3} \left(\ln \frac{1}{\sqrt{\eta}} \right)^{1/3} \beta\alpha^{-2/3}S. \quad (35)$$

Then K spikes are stable if $K < K_c$. Example: $\alpha = 1, \gamma = 2, \varepsilon = 0.08, D = 1$.



We get $S = 16$, $K_c \approx 10.19$. Starting with random initial conditions, the end state consists of $K = 7.5 < K_c$ hot-spots [counting boundary spots with weight $1/2$ and corner spots with weight $1/4$], in agreement with the theory.

References (available for download from my website):

- J. Breslau, T. Chaturapruek, D. Yazdi, S. McCalla and T. Kolokolnikov, *Incorporating Levi flights into a model of crime*, *SIAM J.Appl.Math* 2013
- T. Kolokolnikov, M. Ward and J. Wei, *The Stability of Steady-State Hot-Spot Patterns for a Reaction-Diffusion Model of Urban Crime*, DCDS-B, 2014